

RESEARCH

Open Access



The soluble epoxide hydrolase inhibitor TPPU alleviates A β -mediated neuroinflammatory responses in *Drosophila melanogaster* and cellular models of alzheimer's disease

Xiaowen Sun^{1,2}, Hongxiang Liu^{1,2}, Wei Li^{1,2}, Lin Li^{1,2}, Qian Tian^{1,2}, Qingyang Cao^{1,2}, Yun Meng^{1,2}, Yan Shen^{1,2}, Fengyuan Che^{1,2}, Joanna C. Chiu³, Jixu Yu^{1,2*} and Bruce D. Hammock^{4*}

Abstract

Background Alzheimer's disease (AD) is a common neurodegenerative disease, and its pathogenesis is closely associated with neuroinflammation. The control of neuroinflammation in AD is the focus of current research. Soluble epoxide hydrolase (sEH) protein is increased in the brain tissues of patients with AD and has been targeted by multiple genome wide association studies as a prime target for treating AD. Since sEH induces nerve inflammation by degrading epoxyeicosatrienoic acids (EETs), application of sEH inhibitor and sEH gene knockout are effective ways to improve the bioavailability of EETs and inhibit or even resolve neuroinflammation in AD. 1-trifluoromethoxyphenyl-3-(1-propionylpiperidin-4-yl) urea (TPPU) is a potent sEH inhibitor that has been shown to be effective in preclinical animal models of a variety of chronic inflammatory diseases. This study aims to further explore whether TPPU can alleviate AD neuroinflammation.

Methods We established an A β 42-transgenic *Drosophila melanogaster* model using the galactose-regulated upstream promoter element 4 (GAL4) / upstream active sequence (UAS) expression system and investigated the protective and anti-neuroinflammatory effects of TPPU against A β toxicity. We detected behavioral indexes (survival time, crawling ability, and olfactory memory) and biochemical indexes malondialdehyde (MDA) content and superoxide dismutase (SOD) activity in brain tissues of A β 42 transgenic flies. Finally, we explored the anti-neuroinflammatory effect of TPPU and its possible mechanism by stimulating cocultures of human SH-SY5Y cells and HMC3 cells with A β (25–35) to model neuronal cell inflammation, and evaluated the cells by fluorescence microscopy, ELISA, Western Blot, and Real-time PCR.

Results We found that TPPU improved the survival time, crawling ability, and olfactory memory of A β 42-transgenic flies. We also observed reduction of MDA content and elevation of SOD activity in the brain tissues of these flies. In human cell models, we found that TPPU improved cell viability, reduced cell apoptosis, decreased lipid oxidation,

*Correspondence:

Jixu Yu

yujixu@163.com

Bruce D. Hammock

bdhammock@ucdavis.edu

Full list of author information is available at the end of the article



© The Author(s) 2025. **Open Access** This article is licensed under a Creative Commons Attribution-NonCommercial-NoDerivatives 4.0 International License, which permits any non-commercial use, sharing, distribution and reproduction in any medium or format, as long as you give appropriate credit to the original author(s) and the source, provide a link to the Creative Commons licence, and indicate if you modified the licensed material. You do not have permission under this licence to share adapted material derived from this article or parts of it. The images or other third party material in this article are included in the article's Creative Commons licence, unless indicated otherwise in a credit line to the material. If material is not included in the article's Creative Commons licence and your intended use is not permitted by statutory regulation or exceeds the permitted use, you will need to obtain permission directly from the copyright holder. To view a copy of this licence, visit <http://creativecommons.org/licenses/by-nc-nd/4.0/>.

inhibited oxidative damage, thus playing a neuroprotective role. The inflammatory cytokines tumor necrosis factor- α (TNF- α), interleukin-1 β (IL-1 β), interleukin-6 (IL-6) and interleukin-18 (IL-18) were downregulated, and the mRNA expression of the M2 microglia markers CD206 and SOCS3 were upregulated by TPPU; thus, TPPU inhibited neuroinflammatory responses. TPPU exerted neuroprotective and anti-inflammatory effects by decreasing the protein expression of the sEH-encoding gene EPHX2 and increasing the levels of 11,12-epoxyeicosatrienoic acid (11,12-EET) and 14,15-epoxyeicosatrienoic acid (14,15-EET). The inhibitory effect of TPPU on A β (25–35)-mediated neuroinflammation was associated with inhibition of the toll like receptor 4 (TLR4)/nuclear transcription factor- κ B (NF- κ B) pathway and p38 mitogen activated protein kinases (MAPK)/NF- κ B pathway.

Conclusions We report that the sEH inhibitor TPPU exerts neuroprotective and anti-neuroinflammatory effects in AD models, and it is expected that this drug could potentially be used for the prevention and treatment of AD.

Keywords Alzheimer's disease, Neuroinflammation, TPPU, Neuroprotection, *Drosophila melanogaster*, Cell

Introduction

Alzheimer's disease (AD) is the most common neurodegenerative disease characterized by dementia. Patients with AD initially exhibit memory impairment, gradually develop mental and behavioral abnormalities, eventually lose the ability to care for themselves, and ultimately die. Pathologically, AD is characterized by the accumulation of extracellular amyloid plaques, intracellular neurofibrillary tangles and neuroinflammation, which cause neuronal damage and lead to neurodegeneration [1, 2]. As the population grows and ages, the number of people with dementia worldwide will increase from 57.4 million in 2019 to 152.8 million by 2050 [3]. AD is the leading cause of dementia, accounting for 60–80% of dementia cases [4]. AD has emerged as a major health problem worldwide, and there is still no effective treatment for AD despite extensive basic and clinical research and the investment of billions of dollars [5, 6]. Among the various hypotheses regarding the pathogenesis of AD, neuroinflammation is currently the main research focus [7, 8]. The study shows that neuroinflammation plays a key role in the pathogenesis of AD by accelerating cell death and disease progression [9]. Therefore, inhibition of neuroinflammation is a potential strategy for the treatment and prevention of AD. Neuroinflammation is the inflammatory response of the central nervous system, and it includes immune cell infiltration, microglial activation, and proinflammatory cytokine secretion. Studies on neuroinflammation have shown that microglia, astrocytes, and neurons promote neurodegeneration in a synchronized manner [10]. Microglia are important glial cells that are associated with the innate immune response and play a dual role in the central nervous system. They exert beneficial or harmful effects on neighboring neurons by secreting proinflammatory cytokines and neurotrophic factors [11–13]. Overactivation of microglia can cause these cells to transform into the M1 phenotype, which promotes inflammatory factor secretion. M1 microglia release proinflammatory cytokines (such as tumor necrosis factor (TNF), interleukin-1 (IL-1), interleukin-6

(IL-6), interleukin-12 (IL-12), interleukin-17 (IL-17), interleukin-18 (IL-18), and interleukin-23 (IL-23)), free radicals (such as inducible nitric oxide synthase (iNOS) and reactive oxygen species (ROS)). These secreted factors can block neuronal differentiation, inhibit microglial phagocytosis, and cause cell damage by activating nuclear factor κ B and promoting A β accumulation [11, 12]. In contrast, M2 microglia exhibit an anti-inflammatory phenotype and can secrete anti-inflammatory cytokines (such as interleukin-4 (IL-4), interleukin-10 (IL-10), and interleukin-13 (IL-13)), neurotrophic growth factors (such as glial cell-derived neurotrophic factor (GDNF) and brain-derived neurotrophic factor (BDNF)), and growth factors (such as insulin-like growth factor (IGF-1), transforming growth factor- β (TGF- β), fibroblast growth factor (FGF) and colony stimulating factor (CSF1)) [14]. In the early stages of AD, activated microglia play an active role in clearing A β through phagocytosis. However, as AD progresses, microglia become less efficient at clearing A β and begin to have negative effects on the brain, which eventually results in the accumulation of A β and the deposition of extracellular amyloid plaques. This constantly stimulates microglial activation, which leads to neuroinflammation. A vicious cycle of inflammation is established among A β accumulation, microglial activation, and microglial inflammatory mediator secretion, which enhances A β deposition and neuroinflammation [15]. Therefore, blocking this vicious cycle may be an important strategy to stop neurodegeneration in AD.

In recent years, increasing research has shown that epoxy fatty acids (EpFAs) such as epoxyeicosatrienoic acids (EETs) are closely related to the development of AD by resolving neuroinflammation. EpFAs are mainly produced from intracellular long chain polyunsaturated fatty acids (PUFAs), and this reaction is catalyzed by cytochrome P450 oxidases. For example, EETs are regioisomeric epoxides of arachidonic acid and have multiple effects in nerve tissues, such as neuroprotective, anti-inflammatory, anti-atherosclerosis, cerebrovascular

protective, angiogenesis promoting, neurohormone release promoting, and cell proliferation promoting effects [16, 17]. However, EETs are rapidly degraded by the soluble epoxide hydrolase (sEH) enzyme into the corresponding more polar diols or dihydroxy eicosatrienoic acids and lose their inflammation resolving activity. These diols tend to move out of cells and can be rapidly conjugated. Thus, they perform very limited functions in the body and may have proinflammatory activities acting to increase macrophage mobility. Therefore, applying sEH inhibitors or knocking out the sEH gene is an effective way to improve the bioavailability of EETs [18].

sEH is a bifunctional enzyme with hydrolytic activity in its C-terminal domain and lipid phosphatase activity in its N-terminal domain [19]. In the human nervous system, sEH is mainly found in the cytoplasm of neurons, oligodendrocytes, astrocytes, modified ependymal cells and medium arteriole smooth muscle cells [20]. Recently, increasing the concentration of EETs by blocking the hydrolysis of sEH has been used to ameliorate diseases that are associated with chronic injury to the central nervous system [21–25]. In Parkinson's disease (PD), it has been found that overexpression of sEH in the striatum significantly enhances 1-methyl-4-phenyl-1,2,3,6-tetrahydropyridine (MPTP)-induced neurotoxicity, but the lack of or inhibition of sEH can prevent the loss of dopamine neurons and alleviate MPTP-induced motor disorders [22, 23]. A study on cerebral hemorrhage showed that both sEH gene deletion and pharmacological inhibition could significantly reduce the inflammatory response, blood-brain barrier permeability and neurodegeneration after cerebral hemorrhage [24]. An animal study on AD showed that the injection of a high concentration of 14,15-epoxyeicosatrienoic acid (14,15-EET) (200 ng/ml) into the hippocampus reverses the deposition of A β in the brains of 6-month-old male 5 \times FAD mice, although the mechanism underlying this effect is unclear. This finding highlights the therapeutic potential of EpFA such as 14,15-EET in preventing or delaying the development and progression of AD [25]. Although relevant studies have reported that inhibiting sEH can alleviate AD in multiple animal and cell models, it is still unclear whether inhibiting sEH can reduce neuroinflammation, neuronal death, and oxidative stress in AD. Furthermore, the mechanism by which inhibition of sEH ameliorates AD remains unknown [26, 27]. TPPU is a new type of sEH inhibitor with a longer half-life and higher efficacy; it is the most common sEH inhibitor used in experimental studies [28]. Therefore, we proposed to test 1-trifluoromethoxyphenyl-3-(1-propionylpiperidin-4-yl) urea (TPPU) as a drug for treating AD and to investigate whether it exerts anti-neuroinflammatory effects. The short generation time and high fecundity of flies make it possible to conduct rapid life-span and behavior

screening in large cohorts. The key neurodegenerative and neuroinflammatory signal cascades in flies are evolutionarily conservative, which is beneficial to gene-function verification. Their simplicity, speed, and genetic precision make them indispensable for dissecting conserved pathways and prioritizing targets for human studies. We first examined the effects of TPPU on transgenic *D. melanogaster* expressing A β 42, a common fly model of AD. Human cell models are directly derived from human body, and their gene expression, metabolic pathway, signal transduction and other characteristics are highly consistent with the human environment. Controlled in vitro conditions allow precise dose- and time-course studies, as well as targeted genetic or pharmacological manipulations. Human-derived cells are the core tools to study human biology and diseases, especially in drug development, precision medicine and mechanism research. Its core value lies in restoring the real environment of human body to the greatest extent. The anti-neuroinflammatory effect of TPPU and the possible underlying mechanism were further elucidated in human SHSY5Y cells, HMC3 cells, and neuroglia that were treated with A β (25–35).

Materials and methods

Drosophila melanogaster strains and genetic cross

Wild type (w^{1118}) and Arc2E arc2E/arc2E; +/-red/upstream active sequence (UAS)-A β 42 mutant strains of *D. melanogaster* was purchased from Shanghai Chinese Academy of Sciences. *elav*-galactose-regulated upstream promoter element 4 (GAL4) line driving pan-neuronal expression was from the State Key Laboratory of Medical Genetics, Central South University. The GAL4/UAS system [29, 30] was used to express A β 42 pan-neuronally in fly brains, male progenies that were generated by crossing *elav*-GAL4 female flies and w^{1118} male flies were used as the control group, while male progenies that were produced by crossing *elav*-GAL4 female and A β 42 male flies were used as the experimental group.

Preparation of TPPU-treated fly culture medium

The TPPU stock solution was prepared by dissolving 5 mg TPPU (GC15387, GLPBIO, USA) in 200 μ l DMSO. TPPU working solutions were then prepared at concentrations of 1 μ M, 10 μ M, 15 μ M and 20 μ M. The final concentration of DMSO was carefully maintained below 0.1% to avoid causing toxic damage to the flies. A total of 20.87 g culture medium (ingredients: 81.5 g/l sucrose, 9.2 g/l yeast powder, 1.3 g/l sodium benzoate, 108.5 g/l corn flour, 8.2 g/l agar) was dissolved and boiled in 110 ml distilled water, and then 0.65 ml propionic acid and TPPU working solutions were added and mixed well. Media for rearing larval flies containing different concentrations of TPPU were prepared, and the media were divided into

sterilized culture vials while hot. We stored the culture medium in a refrigerator at 4 °C for use. The media that were used for the control and experimental groups were supplemented with the same concentration of DMSO to ensure that the two groups can be compared.

The culture condition of flies

Fly cultures were maintained at a density of twenty adults per vial and were placed vertically in flies' incubator. Flies were maintained at a constant temperature of 25 °C, in controlled humidity of 50%~60%, and under 12-h light and 12-h dark light cycles. Fly media was replaced with fresh media every 3 days.

To assay the lifespan of flies [29]

We measured the lifespan of adult flies to study the effect of A β toxicity on the adult fly's lifespan and to determine whether TPPU can improve the lifespan of flies with A β deposits. The newly emerged adult first generation males were collected within 48 h, placed in a culture vial (twenty flies/vial, five vial), and incubated in an incubator at 25 °C and 50%~60% humidity. The medium was changed every 3 days, and each vial was labeled with the date and strain. The number of dead flies was counted when the medium was changed. If there was contamination, the medium was replaced. It should be noted that only the survival time of flies that died naturally were counted; the survival times of flies that escaped, drowned, were exposed to excessive anesthetization, adhered, or experienced other unnatural deaths were not recorded. The assay ended when all the flies had died.

The crawling ability of flies [30]

The crawling ability of the adult flies were performed to observe the effect on the physiological ability to crawl against gravity as well as disorders of muscle movement [30]. After hybridization, the male offspring were collected, twenty adult flies were placed in each vial, and the medium was changed every 3 days. A clean culture vial with a height of 12 cm and an inner diameter of 2.5 cm was selected as the crawling vial, and it was divided into three sections: the top, middle, and bottom sections. A total of one hundred adult flies were collected from each group and divided into five crawling vials. After CO₂ anesthesia, the adult flies were placed into the crawling vial and maintained for 15 min, and their crawling ability was assessed. During the test, the flies were shaken down to the bottom of the vial at the same time and then allowed to crawl freely. After 15 s, the numbers of flies in the top, middle, and bottom sections were counted. After each measurement, the flies were allowed to recover their strength for 15 min and were assessed again. The crawling ability of flies at 7, 14 and 21 days was investigated.

The average number and percentage of flies in each section were calculated.

To assay the olfactory memory of flies

The flies olfactory memory defect experiment in adult flies was conducted to observe the effect on the olfactory sense [31]. Each group of adult flies (twenty flies/group) was starved for 2 h in an empty culture vial and then transferred to a 1000 ml beaker. Two 50 ml centrifuge tubes with holes were placed in the beaker, and one tube was directly placed in a banana. The flies in this experiment can smell bananas, and the adult flies in this experiment could directly eat the banana once they entered the centrifuge tube through the hole. The other tube contained banana wrapped with gauze, and the flies could smell this banana but could not eat it. The number of flies that entered the barrier-free centrifuge tube was recorded every hour for 12 h.

Malondialdehyde (MDA) content in brain tissues of flies

The effect on lipid peroxidation in brain tissues of flies was determined by measuring the MDA content. The brain tissues of flies were homogenized with normal saline at a 1:10 (weight: volume) ratio. The MDA content in brain tissues were measured using a commercially available kit (A003-1-1, Nanjingjiancheng, China) according to the manufacturer's instructions. Determine the absorbance of MDA at 532 nm with enzyme-labeled instrument (SpECTRAMAX-M5, USA). The data are expressed as absorbance after protein content normalization.

Superoxide dismutase (SOD) activity in brain tissues of flies

SOD activity was measured to observe the effect on the anti-peroxidation damage capacity of flies. SOD activity was measured by ice bath homogenization at the ratio of flies' brain tissue mass (g): extraction liquid volume (ml) (1:10). We measured the SOD activity in flies brain tissues with commercially available kits (BC0175, Solarbio, Beijing, China) according to the manufacturer's instructions. SOD absorbance was measured at a wavelength of 560 nm. The data are expressed as absorbance after protein content normalization.

A β (25–35) and TPPU preparation

Amyloid β -protein (25–35) amide (GA20745, GLPBIO, USA) was dissolved in sterile distilled water at a concentration of 2.5 mM. To obtain a higher solubility, the tube was heated at 37 °C and shaken for a while by ultrasonication. Then, the A β (25-35) solution was incubated in a 37 °C incubator for 72 h and lightly mixed to promote aggregation.

The TPPU stock solution was prepared by dissolving 5 mg TPPU (GC15387, GLPBIO, USA) in 200 μ l DMSO,

and then the stock solution diluted into 0.1 μM , 1 μM , and 10 μM TPPU working solutions in cell experiments.

Human cell cultures

SH-SY5Y cells (CL0278, Fenghuishengwu, China) are human neuroblastoma cells. These cells were cultured in medium (MEM) (C11095500BT, Gibco, USA) supplemented with 10% FBS (BC-SE-FBS06 C, Bio Channel, Nanjing, China) and 1% penicillin-streptomycin solution (S110 JV, Basal Media, China).

HMC3 cells (ATCC CRL-3304, Pricella, China) are human microglia. These cells were cultured in MEM (including NEAA) (PM150410, Pricella, China) supplemented with 10% FBS (BC-SE-FBS06 C, Bio Channel, Nanjing, China) and 1% penicillin-streptomycin solution (S110 JV, Basal Media, China).

During coculture, HMC3 cells were pretreated with 1 μM TPPU for 3 h and then incubated with 30 μM A β (25–35) for 48 h. The medium was replaced with fresh MEM (including NEAA), and the MEM was collected after 24 h. The collected MEM was centrifuged, added to SH-SY5Y cells, and incubated for 48 h for further analysis. All the cells were cultured at 37°C in 5% CO₂.

CCK-8 cell viability assay

Cell viability was determined by CCK-8 (Cell Counting Kit-8) assay. The cell density of SH-SY5Y cells or HMC3 cells was adjusted to 4×10^3 cells/well, and 100 μl /well was seeded in 96-well plates. Intervene after cell adhesion, 10 μl CCK-8 solution (GK10001, GLPBIO, USA) was added to each well and then incubated for 4 h. The OD value of each well was measured at 450 nm. Cell viability = (OD experimental group - OD blank group)/(OD control group - OD blank group).

Crystal Violet staining to test cellular morphology in SH-SY5Y cells

To observe the changes in cell number and axon length, SH-SY5Y cells were stained with crystal violet. After counting the cells, SH-SY5Y cells were seeded in 6-well plates at a cell density of 3×10^5 cells/well (2 ml/well). After the cells adhered, the treatment group was pretreated with medium containing 0.1 μM TPPU for 3 h. The control group and A β (25–35) group were pretreated with medium containing 0.1 μM DMSO. After incubation for 3 h, the A β (25–35) group and treatment group were treated with 25 μM A β (25–35) solution, and incubation was continued for 48 h. The medium in the 6-well plates was discarded, the cells in each well were gently rinsed 3 times with 1 \times PBS, and then 4% paraformaldehyde (1 ml) was added to each well to fix the cells for 20 min. Then, the formaldehyde solution was discarded, and 1 \times PBS was added to wash the cells 3 times for 5 min each. Then, 1% crystal violet solution (G1063, Solarbio,

Beijing, China) was added in a volume of 500 μl /well, the cells were stained for 10 min, the crystal violet solution was discarded, the cells were washed with 1 \times PBS 3 times for 5 min each, and finally, the cells were viewed under a microscope and photographed.

Hoechst 33258 staining to test cell apoptosis in SH-SY5Y cells

Hoechst 33258 staining was used to analyze changes in apoptosis. SH-SY5Y cells or cocultured SH-SY5Y cells were seeded at a cell density of 3×10^5 cells/well in 6-well plates on a slide, and the cells were fixed in 4% paraformaldehyde for 20 min after treatment. After washing with 1 \times PBS 3 times for 5 min each, 10 $\mu\text{g}/\text{ml}$ Hoechst 33258 staining solution (C0021, Solarbio, Beijing, China) was added and incubated in a 37°C incubator for 20 min. After washing with 1 \times PBS 3 times for 5 min each, a drop of anti-fluorescence attenuation mounting medium (S2100, Solarbio, Beijing, China) was added, and the stained cells were observed under a fluorescence microscope. At least 200 cells from three fields were randomly selected for detection and quantification in each experiment, and the percentage of apoptotic cells was calculated with the following formula: apoptotic cells/total number of cells $\times 100$.

MDA content and SOD activity in the cells

The MDA content and SOD activity in the cells were determined. After centrifugation, the medium was discarded, 1 mL of extraction solution was added for every 5 million cells, the cells were homogenized by ultrasonication and centrifuged at 8000 g and 4°C for 10 min, and finally the supernatants were collected for analysis. We used a commercially available Malondialdehyde (MDA) Content Assay Kit (BC0025, Solarbio, Beijing, China) and Superoxide Dismutase (SOD) Activity Assay Kit (BC0175, Solarbio, Beijing, China) to measure the MDA and SOD levels in cells according to the manufacturer's instructions.

ROS to test oxidative stress in cells

The ROS Assay Kit - Highly Sensitive DCFH-DA- (R252, Dojindo, China) was used to detect oxidative stress. Cells (2×10^4 cells/well) were seeded in a 24-well plate. After the cells had adhered, they were pretreated with 1 μM TPPU for 3 h and then incubated with 30 μM A β (25–35) for 48 h. The culture medium was removed, the cells were washed with HBSS buffer twice, Highly Sensitive DCFH-DA Dye working solution was added, and cells were cultured for 30 min at 37°C and 5% CO₂ in an incubator. The working solution was removed, the cells were washed with HBSS buffer twice, HBSS buffer was added again, and the cells were observed with a fluorescence microscope.

Interleukin-1 β (IL-1 β), 11,12-epoxyeicosatrienoic acid (11,12-EET), and 14,15-EET levels were determined by ELISA

The homogenized cells were centrifuged to remove cell debris. According to the manufacturer's instructions, IL-1 β levels were measured using the Human IL-1 β High Sensitivity ELISA Kit (EK101BHS-AWI, MULTI SCIENCES, China). The optical density (450 nm and 570 nm) of experimental wells was compared with the standard curve.

The medium of homogenized cells was collected, repeatedly frozen at -20°C and thawed 3 times, and then filtered by glass fiber for analysis. An 11,12-epoxide eicosatrienoic acid (11,12-EET) ELISA kit (MM 927114O1, Meimian, Jiangsu, China) and a 14,15-epoxidized eicosatrienoic acid (14,15-EET) ELISA Kit (MM 927107O1, Meimian, Jiangsu, China) were used to measure the levels of 11,12-EET and 14,15-EET according to the manufacturer's instructions. The absorbance (OD value) was measured at 450 nm, and 11,12-EET and 14,15-EET levels in the samples were calculated according to the standard curve.

Western blot

Human cells were washed 3 times with $1\times$ PBS, and the cells were lysed with RIPA lysis buffer (R0010, Solarbio, Beijing, China) supplemented with protease inhibitor mixture (P6730, Solarbio, Beijing, China) and PMSF (P0100, Solarbio, Beijing, China). The lysed cells were collected and centrifuged at 12,000 rpm and 4°C for 20 min. After the protein concentration was determined with a BCA protein detection kit (P0010, Beyotime, China), the protein was denatured in loading buffer at 100°C for 10 min. An equal amount of protein was resolved with a 10–12% SDS-PAGE gel and then transferred to a polyvinylidene fluoride (PVDF) membrane (ISEQ00010, Immobilon, USA). After incubation with 5% skim milk (P1622, Applygen, China) for 2 h, the PVDF membrane

was incubated with primary antibodies overnight at 4°C . Antibodies include rabbit anti-TNF- α (ER65189, HUABIO Antibodies, China, 1:1000), rabbit anti-EPHX2 (HA721056, HUABIO Antibodies, China, 1:500), rabbit anti-TLR4 (AF7017, Affinity Biosciences, China, 1:1000), rabbit anti-MyD88 (ET1610-81, HUABIO Antibodies, China, 1:1000), rabbit anti-p38 MAPK (#8690, Cell Signaling Technology, USA, 1:1000), rabbit anti-P-p38 MAPK (#4511, Cell Signaling Technology, USA, 1:1000), rabbit anti-NF- κ B p65 (ET1603-12, HUABIO Antibodies, China, 1:500), rabbit anti-P-NF- κ B p65 (#3033, Cell Signaling Technology, USA, 1:1000), and rabbit anti- β -actin (#4970, Cell Signaling Technology, USA, 1:1000) antibodies. The PVDF membranes were washed with $1\times$ TBST 3 times and incubated with HRP-conjugated goat anti-rabbit IgG antibody (HA1001, HUABIO Antibodies, China) for 2 h. The protein bands were detected by an Ultra High Sensitivity ECL Kit (GK10008, GLPBIO, USA). β -actin (#4967, Cell Signaling Technology, USA, 1:1000) used as loading control. ImageJ software was used to quantify the protein expression levels.

Real-time PCR for gene expression analysis in cells

Real-time PCR was used to measure the mRNA expression of inflammatory markers in human cells. Total RNA was extracted from human cells by the TRizol method (T9424, SIGMA, USA). RNA concentrations were measured using a spectrophotometer (Thermo Fisher Scientific, USA). Reverse transcription was performed using Evo M-MLV RT Premix for qPCR (AG11706, AG, China), and cDNA was synthesized according to the manufacturer's instructions. SYBR[®]Green Premix Pro Tag HS qPCR kit (AG11701, AG, China) was used to perform quantitative PCR amplification of the designated genes on a fluorescence quantitative PCR instrument (A25619 CN, Thermo Fisher Scientific, USA). After initial denaturation (95°C , 30 s), amplification was performed 40 times at 95°C for 5 s and 60°C for 30 s. GAPDH was used as the internal reference. The relative gene expression was calculated by the $2^{-\Delta\Delta\text{Ct}}$ method. The human cell primer sequences are shown in Table 1.

Table 1 Primer sequences to assay gene expression in human cells

Gene	Forward primer (5'-3')	Reverse primer (5'-3')
TNF	CCTCTCTAATCAGCCCTCTG	GAGGACCTGGAGTA-GATGAG
IL-1 β	GCCAGTGAAATGATGGCTTATT	AGGAGCACTTCATCT-GTTTAGG
IL-6	CACTGGTCTTTTGGAGTTTGAG	GGACTTTTGACTCATCT-GCAC
IL-18	GCTGAAGATGATGAAAACCTGG	CAAATAGAGGCC-GATTTCCCTTG
SOCS3	CTTCTCTGCAGAGCGATC	ATGTAATAG-GCTCTCTGGGGG
CD206	GACGTGGCTGTGGATAAATAAC	CAGAAGACGCATGTA-AAGCTAC
GAPDH	CAGGAGGCATTGCTGATGAT	GAAGGCTGGGCTCATT

Statistical data analysis

All the experiments were repeated $n \geq 3$ times, and all the data were analyzed using SPSS 26.0 (SPSS Inc., Chicago, IL, USA) with Student's *t* test or one-way analysis of variance (ANOVA) and Bonferroni post event test. The data are expressed as the mean \pm SEM. GraphPad Prism 9 software (GraphPad Software Inc., San Diego, CA, USA) was used to generate the graphs. Differences were considered statistically significant when $P < 0.05$ (* $P < 0.05$, ** $P < 0.01$, *** $P < 0.001$; # $P < 0.05$, ## $P < 0.01$, ### $P < 0.001$).

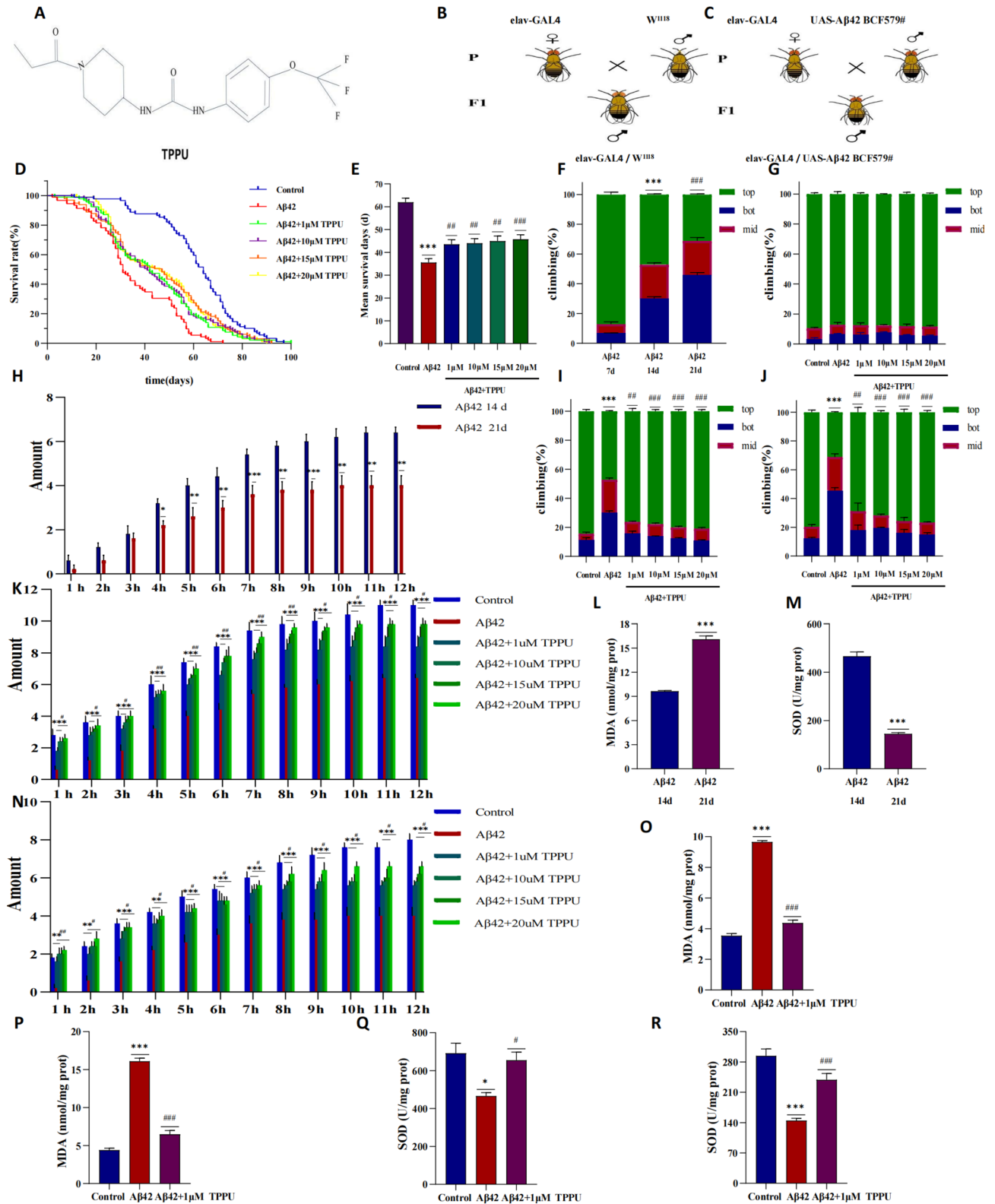


Fig. 1 (See legend on next page.)

(See figure on previous page.)

Fig. 1 TPPU improve the behavioral performance and ameliorate oxidative damage of A β 42-expressing flies. **A** Chemical structure of TPPU. **B** Flies cross breed of the control group. **C** Flies crossbreed of A β 42-expressing flies' group. **D** Flies lifespan curve. **E** Flies survival time. **F** Crawling ability of A β 42-expressing flies at 7 d, 14 d and 21 d of age. *** P <0.001 indicates significant differences between the 7 d and 14 d groups; ### P <0.001 indicates significant differences between the 14 d and 21 d groups. **G** The crawling ability of 7-d-old flies. **H** Olfactory memory between A β 42-expressing flies at 14 d and 21 d of age. * P <0.05, ** P <0.01 and *** P <0.001. **I** The crawling ability of 14-d-old flies. **J** The crawling ability of 21-d-old flies. **K** Olfactory memory experiment with flies at 14 d of age. **L** MDA content in brain tissue of A β 42-expressing flies at 14 d and 21 d of age. *** P <0.001. **M** SOD activity in brain tissue of A β 42-expressing flies at 14 d and 21 d of age. *** P <0.001. **N** Olfactory memory experiment of flies at 21 d of age. **O** MDA content in brain tissues of 14-d-old flies. **P** MDA content in brain tissues of 21-d-old flies. **Q** SOD activity in brain tissues of 14-d-old flies. **R** SOD activity in brain tissues of 21-d-old flies. **E, G, I-K, N-R** * P <0.05, ** P <0.01 and *** P <0.001 indicate significant differences in A β 42-expressing flies group compared with the control group. # P <0.05, ## P <0.01 and ### P <0.001 indicate significant differences in A β 42-expressing flies group compared with the TPPU-treated group. $n=3$, means \pm SEMs. The data were analyzed using Student's t test or one-way analysis of variance (ANOVA) and Bonferroni post event test

Results

TPPU improves behavioral performance of A β 42-transgenic flies

To determine the effect of TPPU (Fig. 1A) in AD, we leveraged a transgenic fly strain that expresses A β 42 pan-neuronally as an AD model (Fig. 1C). Control flies were generated by crossing male *w¹¹¹⁸* flies with female flies carrying the *elav-GAL4* transgene (Fig. 1B). As expected, the lifespan of A β 42-expressing flies was decreased compared to that of the control group. Different concentrations of TPPU (1 μ M, 10 μ M, 15 μ M, or 20 μ M) could prolong the lifespan of A β 42-expressing flies (Fig. 1D, E). The results showed that TPPU protected against A β toxicity and could improve the survival time of A β 42-expressing transgenic flies. Due to A β toxicity, the crawling ability of A β 42-expressing flies showed significant deficiency compared to control flies. The results showed that A β 42-expressing flies showed a more obvious decline in crawling ability with increasing age, which was consistent with the clinical manifestations of human AD (Fig. 1F). On the 7th day, there was no significant change in crawling ability between the A β 42 group and the control group, and there was no significant improvement in crawling ability between the A β 42 flies treated with TPPU (Fig. 1G). On the 14th and 21st days, A β 42-expressing flies exhibited significantly decreased crawling ability compared with the normal group. After treatment with different concentrations of TPPU (1 μ M, 10 μ M, 15 μ M, or 20 μ M), the crawling ability of A β 42-expressing flies was significantly improved (Fig. 1I, J). The results showed that TPPU could improve the crawling ability of aging A β 42-transgenic flies.

The clinical manifestation of AD includes significant memory impairment. We therefore simulated this characteristic by evaluating olfactory memory deficit by investigating whether flies could track a banana odor. Although the number of A β 42-expressing flies that reached and ate the banana increased with as the test progressed, the number in the A β 42-transgenic group was always lower than that in the control group (Fig. 1K, N). The olfactory memory deficit of A β 42-transgenic flies at 21 days of age was more severe than that at 14 days of age, and this feature was more significant as the test progressed, and the

difference was significant after 4 h (Fig. 1H). After treatment with different concentrations of TPPU (1 μ M, 10 μ M, 15 μ M, or 20 μ M), the olfactory memory of A β 42-transgenic flies was improved, and the number of 14 and 21-day-old A β 42-transgenic flies treated with TPPU was higher than that of A β 42-transgenic flies in each test period (Fig. 1K, N). The experiment showed that TPPU could improve the olfactory memory of A β 42-expressing transgenic flies.

In summary, we found that A β 42-expressing flies showed significant behavioral deficiencies compared with control flies. After treatment with different concentrations of TPPU (1 μ M, 10 μ M, 15 μ M, or 20 μ M), the behavioral deficiencies of A β 42-expressing flies were improved, while there was no significant difference among the four treatment groups. Therefore, we selected 1 μ M TPPU as the treatment concentration for subsequent experiments.

TPPU ameliorates oxidative damage in the brain tissues of A β 42-expressing flies

MDA content is an important indicator of potential antioxidant capacity as well as the rate and intensity of lipid peroxidation. The level of SOD indirectly reflects the ability to remove oxygen free radicals and play an important role in the biological antioxidant system [32]. We found that MDA content was increased while SOD activity was significantly decreased in flies that were 21 days old compared with those that were 14 days old (Fig. 1L, M). Similarly, MDA content in brain tissue of A β 42-expressing flies was significantly increased compared with that from control flies (Fig. 1O, P), while SOD activity was decreased (Fig. 1Q, R). After treating these same groups of flies with TPPU, we observed that MDA content was significantly decreased and SOD activity was increased in the brain tissues of A β 42-expressing flies (Fig. 1O-R). We therefore concluded that TPPU improves the antioxidant damage ability of fly brain tissue.

Protective effect of TPPU against A β (25–35)-mediated neurotoxicity in SH-SY5Y cells

TPPU alleviates A β (25–35)-induced cytotoxic effects against SH-SY5Y cells. To demonstrate the

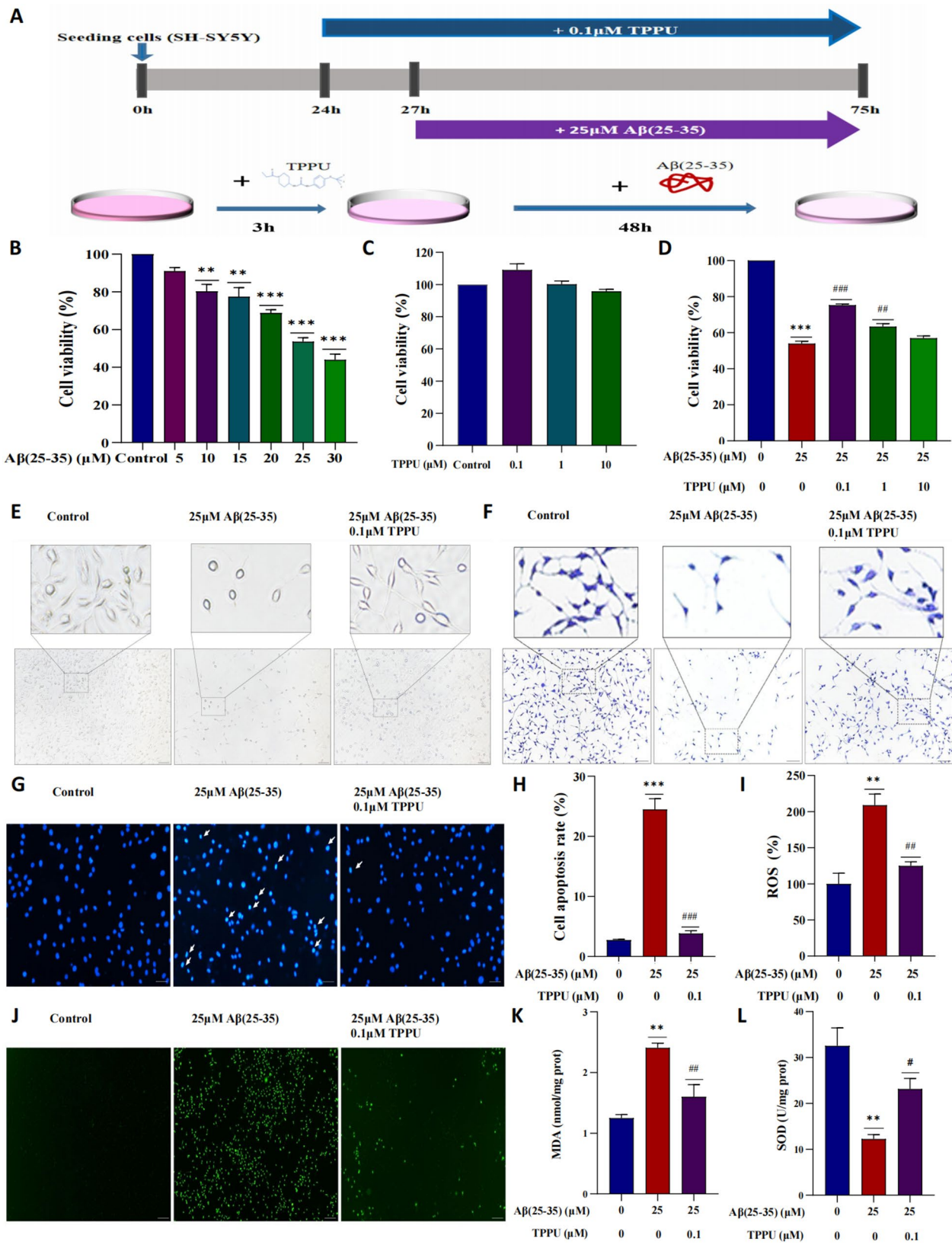


Fig. 2 (See legend on next page.)

(See figure on previous page.)

Fig. 2 TPPU reduces A β (25–35)-mediated neurotoxicity and oxidative damage in SH-SY5Y cells. **A** SH-SY5Y cells experimental design. **B** The effect of different concentrations of A β (25–35) on the viability of SH-SY5Y cells was determined for 48 h by CCK-8. **C** Assessment of TPPU-induced cytotoxicity in SH-SY5Y cells. SH-SY5Y cells were treated with TPPU at different concentrations (0.1 μ M, 1 μ M or 10 μ M) for 48 h. **D** The effect of TPPU pretreatment on the viability of SH-SY5Y cells after treatment with A β (25–35). Cells were pretreated with varying concentrations of TPPU for 3 h followed by 25 μ M A β (25–35) stimulation for 48 h. **E** Morphological changes in SH-SY5Y cells under the microscope. Scale bar = 100 μ m. **F** The morphological changes of SH-SY5Y cells after crystal violet staining. Scale bar = 100 μ m. **G** Hoechst 33258 staining; arrow indicates apoptotic cells. Scale bar = 100 μ m. **H** Quantitative analysis of apoptotic cells that were identified by Hoechst 33258 staining. **I** Average fluorescence intensity of ROS (normalized to the control group). **J** ROS were imaged under a fluorescence microscope; green fluorescence represents the fluorescence intensity of the ROS probe DCFH-DA. Scale bar = 100 μ m. **K** MDA content. **L** SOD activity. The A β (25–35) group was compared with the control group, * P < 0.05, ** P < 0.01 and *** P < 0.001; the A β (25–35) group was compared with the TPPU pretreatment group, # P < 0.05, ## P < 0.01 and ### P < 0.001. n = 3, means \pm SEMs. The data were analyzed using one-way analysis of variance (ANOVA) and Bonferroni post event test

neuroprotective effect of TPPU against A β -induced neurotoxicity, we performed cell viability experiments. The three experimental concentrations (0.1 μ M, 1 μ M and 10 μ M) of TPPU were safe and had no effect on the viability of SH-SY5Y cells (Fig. 2C). 25 μ M A β (25–35) to treat SH-SY5Y cells for 48 h decreased the cell viability by nearly 50% (Fig. 2B). SH-SY5Y cells were pretreated with 0.1 μ M TPPU for 3 h and then stimulated with 25 μ M A β (25–35) for 48 h for subsequent experiments (Fig. 2D).

To observe the effect of A β (25–35) on the morphology of SH-SY5Y cells, three groups of SH-SY5Y cells were exposed to different treatments and photographed under a microscope (Fig. 2E). To observe the morphological changes in SH-SY5Y cells more clearly, crystal violet staining was performed on SH-SY5Y cells (Fig. 2F). The results showed that cells that were stimulated with 25 μ M A β (25–35) showed harmful morphological changes compared with the untreated control group. After A β (25–35) stimulation, the number of cells was significantly reduced, the shape of the cells became rounder and blunter, and the neurite processes shrank and were significantly shortened. However, 0.1 μ M TPPU treatment effectively ameliorated the toxic effects of A β (25–35) on SH-SY5Y cells, the cell number significantly increased, and the axons became longer. The results indicated that TPPU exerted a protective effect against A β toxicity. Neuronal apoptosis is an important pathological feature of AD. Hoechst 33258 fluorescence staining was used to detect apoptosis. After staining normal cells, it could be seen under the fluorescence microscope that the nuclei of the control group were intact, oval, or round-like in shape, with regular edges, and the intracellular fluorescence was uniformly bright and light blue. After SH-SY5Y cells were stimulated with A β (25–35) for 48 h, cell nuclei exhibited many characteristics of apoptosis, such as compact, beaded, or fragmentary appearances, irregular edges, and change in color from blue to white. TPPU significantly inhibited the apoptosis of SH-SY5Y cells stimulated by A β (25–35), and the

number of apoptotic cells was significantly reduced (Fig. 2G, H). It indicated that TPPU exerted a protective effect against A β toxicity.

TPPU alleviates the oxidative damage of SH-SY5Y cells induced with A β (25–35)

The high contents of reactive oxygen species in the brains of AD patients can promote the production of A β and exacerbate the symptoms of AD [33]. We labeled cells with the ROS probe DCFH-DA, and cells that were exposed to A β (25–35) emitted much brighter green fluorescence than control cells. The green fluorescence significantly decreased after TPPU treatment (Fig. 2I, J). This suggests that TPPU can effectively alleviate A β -stimulated oxidative damage in SH-SY5Y cells and that it exerts a protective effect against AD. MDA and SOD are classical indicators of oxidative damage. The level of MDA often indicates the degree of lipid peroxidation in the body. The level of SOD indirectly indicates the oxygen free radical scavenging ability. Compared with the control group, MDA content was significantly increased and SOD activity was significantly decreased after SH-SY5Y cells were stimulated with A β (25–35). MDA content was significantly decreased after TPPU treatment (Fig. 2K), while SOD activity was increased (Fig. 2L). The results showed that TPPU promoted free radical scavenging and prevented lipid peroxidation.

TPPU alleviates the neuroinflammatory response of SH-SY5Y cells induced with A β (25–35)

We used ELISA, Western Blot, and real-time PCR to measure the expression levels of inflammatory cytokines in the control group, A β group and TPPU group. ELISA showed that the IL-1 β levels were significantly higher in the cell culture medium of the A β group than that of the control group, and TPPU effectively reduced the IL-1 β levels in the A β group (Fig. 3C). Western Blot analysis showed that the TNF- α protein levels were increased significantly in the A β group, and TPPU treatment significantly decreased the TNF- α

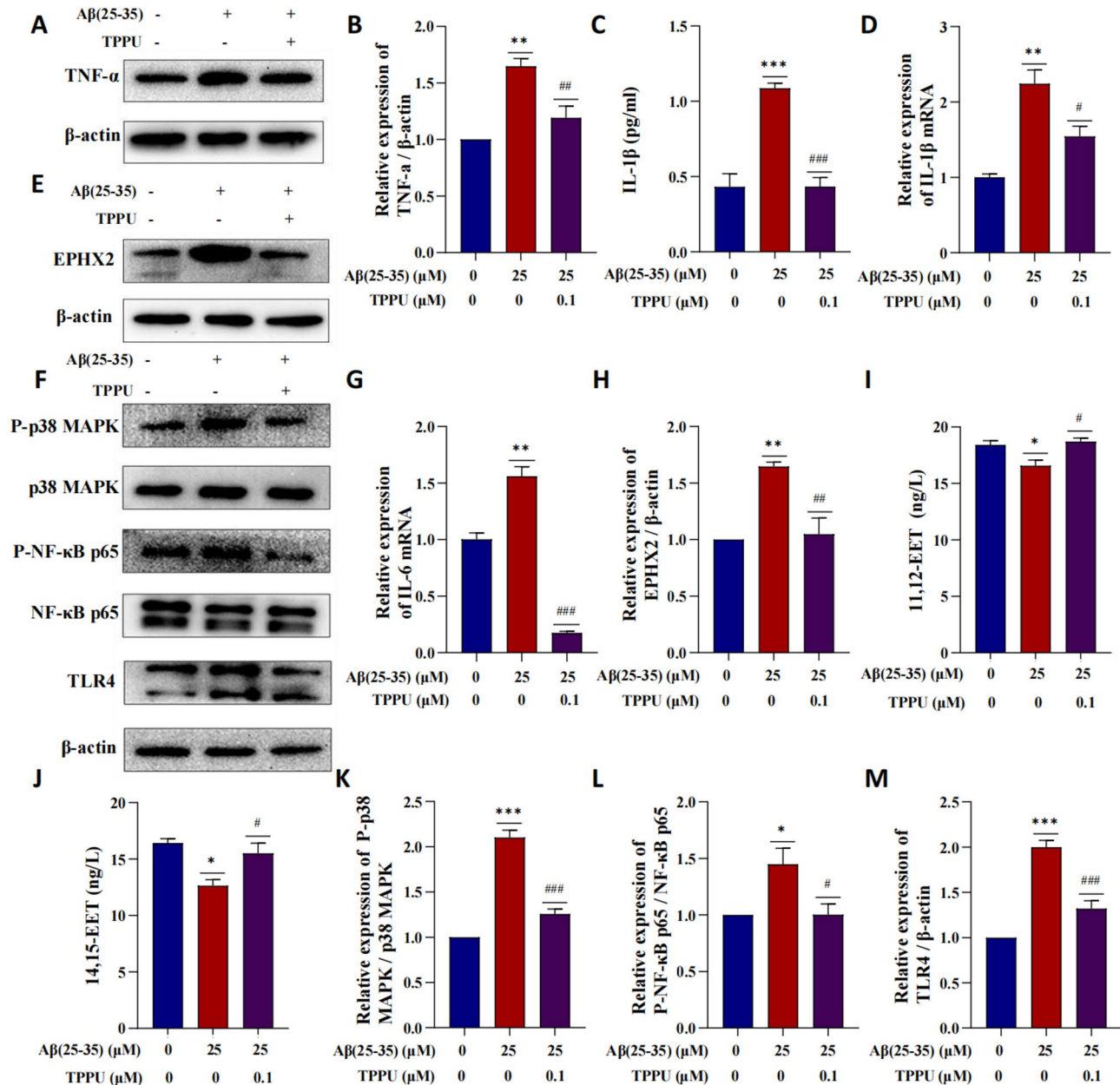


Fig. 3 TPPU against Aβ(25–35)-mediated neuroinflammation in SH-SY5Y cells. The expression levels of TNF-α (A, B), EPHX2 (E, H), P-p38 MAPK (F, K), p38 MAPK (F), P-NF-κB p65 (F, L), NF-κB p65 (F, L) and TLR4 (F, M) in SH-SY5Y cells were analyzed by Western Blot. IL-1β (C), 11,12-EET (I) and 14,15-EET (J) levels in cell culture medium were measured by ELISA. The mRNA expression of IL-1β (D) and IL-6 (G) were measured by real-time PCR. The Aβ(25–35) group was compared with the control group, * $P < 0.05$, ** $P < 0.01$ and *** $P < 0.001$; the Aβ(25–35) group was compared with the TPPU group, # $P < 0.05$, ## $P < 0.01$ and ### $P < 0.001$. $n = 3$, means \pm SEMs. The data were analyzed using one-way analysis of variance (ANOVA) and Bonferroni post event test

protein levels (Fig. 3A, B). Real-time PCR showed that the mRNA expression of IL-1β and IL-6 in the Aβ group was significantly higher than that in the control group, and TPPU treatment decreased the expression of these inflammatory cytokines (Fig. 3D, G). These results suggest that Aβ can exacerbate neuroinflammation and that TPPU can alleviate neuroinflammation in AD and play a neuroprotective role.

TPPU alleviates Aβ-mediated neuroinflammation by increasing EET levels and exerts antineuroinflammatory effects by regulating the TLR4/NF-κB and p38 MAPK/NF-κB signaling pathways in SH-SY5Y cells

The EPHX2 gene encodes sEH, and we measured the expression of the protein that is encoded by the EPHX2 gene by Western Blot. We found that the EPHX2 protein levels were significantly increased in the Aβ group, while

the EPHX2 protein levels were significantly decreased after TPPU treatment (Fig. 3E, H). EETs are an important indicator of sEH. Next, the 11,12-EET and 14,15-EET levels were measured by ELISA. We found that the 11,12-EET and 14,15-EET levels were decreased in the A β group compared with the control group. The 11,12-EET and 14,15-EET levels were increased after TPPU treatment (Fig. 3I, J). This finding suggests that sEH plays an important role in AD pathology. Taken together, these results suggest that TPPU could alleviate A β -mediated neuroinflammation by increasing the EET levels.

To explore how TPPU exerts its anti-neuroinflammatory effect, Western Blot experiments were performed to measure the protein expression of TLR4, NF- κ B p65, P-NF- κ B p65, p38 MAPK, and P-p38 MAPK. There was no significant difference between the protein expression of p38 MAPK and NF- κ B p65 in SH-SY5Y cells stimulated with A β and control cells. While the protein expression levels of P-p38 MAPK, P-NF- κ B p65 and TLR4 were significantly upregulated, these changes were significantly reversed after TPPU treatment (Fig. 3F, K-M). TPPU can effectively inhibit A β -induced NF- κ B activation. These results suggest that TPPU can reduce neuroinflammation. TPPU can reduce A β -mediated cell damage by inhibiting the TLR4/NF- κ B pathway and p38 MAPK/NF- κ B pathway.

TPPU attenuates the A β (25–35)-induced oxidative damage in microglia

Microglia are innate immune cells in the brain. Under physiological conditions, microglia are in a resting state and perform the functions of immune surveillance, immune defense, and tissue repair. When stimulated by inflammation or A β , microglia become activated, and activated microglia secrete cytokines into the extracellular environment, resulting in neurotoxicity to peripheral neurons [34]. We first stimulated HMC3 cells with different concentrations of A β (25–35) (5 μ M, 10 μ M, 15 μ M, 20 μ M, 25 μ M, 30 μ M, or 35 μ M) for 48 h and then measured HMC3 cell viability by CCK-8 assay to determine 30 μ M A β (25–35) for subsequent experiments (Fig. 4B). TPPU (0.1, 1, or 10 μ M) had no negative effect on HMC3 cells (Fig. 4C). The cells were treated with different concentrations of TPPU for 3 h and then stimulated with A β (25–35) (30 μ M) for 48 h. A β (25–35) stimulation did not reduce the viability of HMC3 cells that had been treated with different concentrations of TPPU. Moreover, treatment of HMC3 cells with 1 μ M TPPU had the best effect on preventing A β (25–35) toxicity (Fig. 4D), so 1 μ M TPPU was selected for the treatment of HMC3 cells in follow-up experiments (Fig. 4E).

We verified whether TPPU could alleviate oxidative damage by detecting ROS, MDA and SOD in microglia. ROS can accelerate A β aggregation and the formation of

neurofibrillary tangles. Intracellular ROS production is another marker of microglial activation, and ROS production can in turn induce microglia to secrete more proinflammatory cytokines, thus exacerbating the inflammatory response. Fluorescence microscopy was used to observe whether TPPU could reduce ROS production. The results showed that the number of DCFH-DA-positive cells was significantly increased in microglia that were treated with A β (25–35) for 48 h, while TPPU significantly inhibited the A β (25–35)-induced ROS production (Fig. 4F, G). Therefore, TPPU could alleviate A β (25–35)-induced ROS production in microglia. Through an analysis of MDA content and SOD activity in microglia from different groups, we found that MDA content in microglia treated with A β (25–35) was significantly increased, and SOD activity was significantly decreased. This result indicated that lipid peroxidation was increased, and the ability to scavenge oxygen free radicals was decreased after treatment with A β (25–35) for 48 h. Moreover, MDA content was significantly decreased, and SOD activity was significantly increased in microglia that were treated with TPPU and with A β (25–35) (Fig. 4H, I). This indicated that TPPU could reduce lipid peroxidation and increase antioxidant damage capacity.

TPPU attenuates the A β (25–35)-induced neuroinflammatory response in microglia, promotes the polarization of microglia toward the M2 phenotype

Under conditions of continuous A β stimulation, more microglia polarized toward the proinflammatory M1 phenotype, producing many proinflammatory cytokines, while anti-inflammatory M2 microglia had a decreased ability to alleviate inflammation [35]. Western Blot was used to measure the protein expression of TNF- α were treated with A β (25–35). We found the protein expression of TNF- α was significantly increased (Fig. 5A, B). We used ELISA to measure the IL-1 β levels in the culture media of cells that were treated with A β (25–35), and we found that these levels were significantly increased (Fig. 6C). On the other hand, TNF- α protein and IL-1 β levels were significantly decreased after TPPU treatment (Fig. 5A-C). Additionally, real-time PCR was used to measure the expression of inflammatory cytokines to further verify whether TPPU could decrease the A β -induced inflammatory response in microglia. We found TPPU decreased the mRNA expression levels of TNF, IL-1 β , IL-6, and IL-18 (Fig. 5D-G), The mRNA expression of the M2 markers CD206 and SOCS3 was increased after TPPU treatment (Fig. 5H, J). This result suggested that TPPU could promote the polarization of microglia toward the M2 phenotype, inhibit the over-activation of microglia, and effectively alleviated A β -induced inflammation.

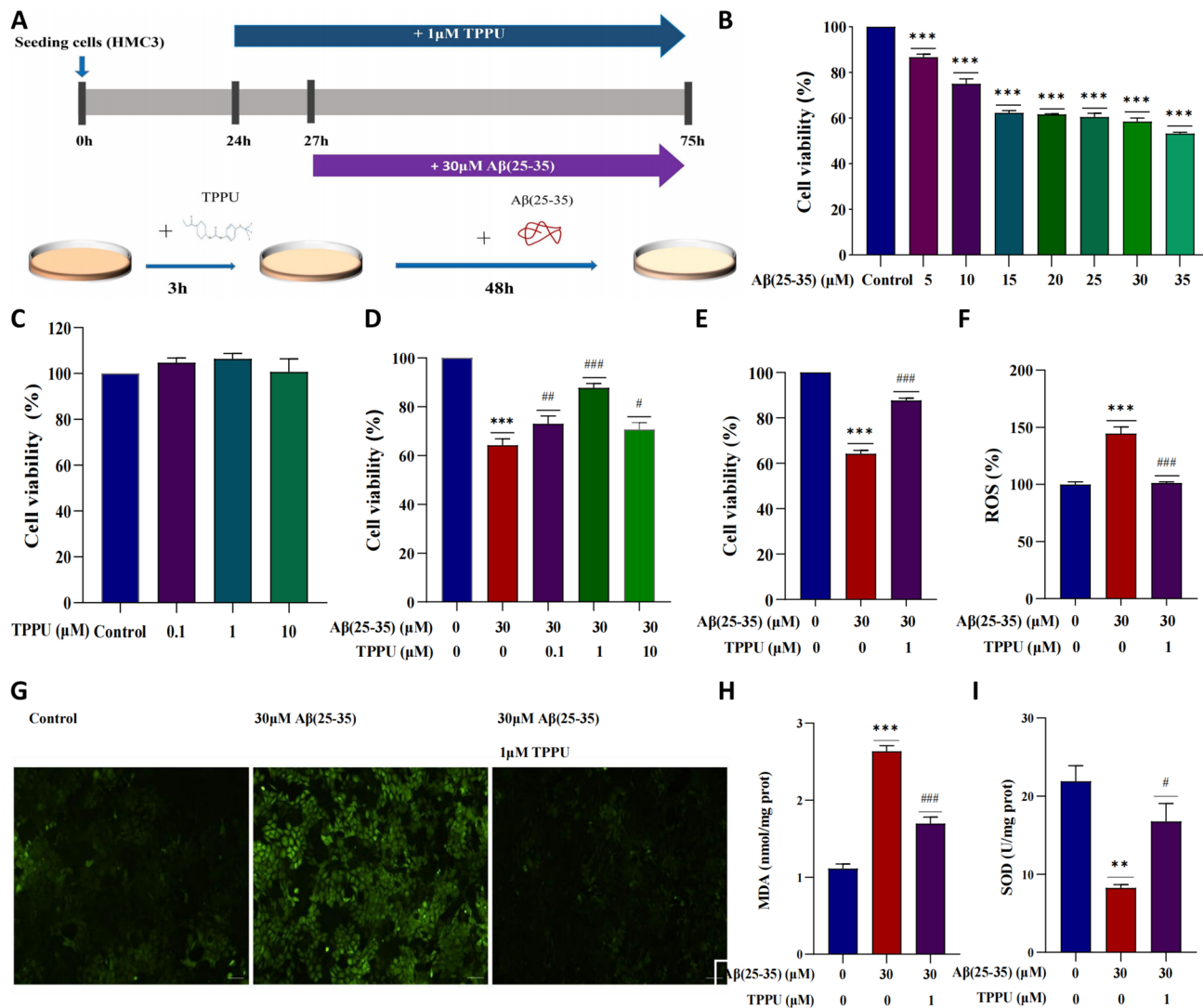


Fig. 4 TPPU reduces Aβ(25–35)-induced oxidative damage in HMC3 cells. **A** Schematic of the HMC3 cell experimental design. **B** The effect of different concentrations of Aβ(25–35) on the viability of HMC3 cells after 48 h was determined by CCK-8 assay. **C** Assessment of TPPU cytotoxicity in HMC3 cells treated with different concentrations of TPPU (0.1 μM, 1 μM or 10 μM) for 48 h. **D** The effect of TPPU pretreatment on the viability of HMC3 cells after treatment with Aβ(25–35). HMC3 cells were pretreated with varying concentrations of TPPU for 3 h followed by 30 μM Aβ(25–35) stimulation for 48 h. **E** HMC3 cells were pretreated with 1 μM TPPU for 3 h and then stimulated with 30 μM Aβ(25–35) for 48 h. **F** Average fluorescence intensity of ROS (normalized to the control group). **G** ROS were imaged under a fluorescence microscope. Green fluorescence represents ROS that were labeled with the ROS probe DCFH-DA. Scale bar = 100 μm. **H** MDA content. **I** SOD activity. The Aβ(25–35) group was compared with the control group, * $P < 0.05$, ** $P < 0.01$ and *** $P < 0.001$; the Aβ(25–35) group was compared with the TPPU pretreatment group, # $P < 0.05$, ## $P < 0.01$ and ### $P < 0.001$. $n = 3$, means \pm SEMs. The data were analyzed using one-way analysis of variance (ANOVA) and Bonferroni post event test

TPPU alleviates the neuroinflammatory response by stabilizing EET levels and exerts antineuroinflammatory effects by regulating the TLR4/MyD88/NF-κB and p38 MAPK/NF-κB signaling pathways in microglia

We investigated whether the protein expression of EPHX2 changes in microglia treated with Aβ(25–35). Western Blot analysis showed that the protein expression of EPHX2 was increased after treatment with Aβ(25–35) and downregulated after treatment with TPPU (Fig. 5I, K). We measured the levels of 11,12-EET and 14,15-EET in the cell culture medium, and we found that these

levels were decreased in the Aβ group and significantly increased in the TPPU group (Fig. 5L, N). Therefore, inhibition of sEH can stabilize the levels of EETs, which exert anti-neuroinflammatory and neuroprotective effects.

TLR4 plays an important role in the process of neuroinflammation. Aβ can bind to TLR4, leading to TLR4 activation, which activates NF-κB through the recruitment of MyD88, and ultimately activates microglia [36]. Activation of the TLR4/MyD88/NF-κB pathway increases the levels of TNF-α, IL-1β, IL-6 and other proinflammatory

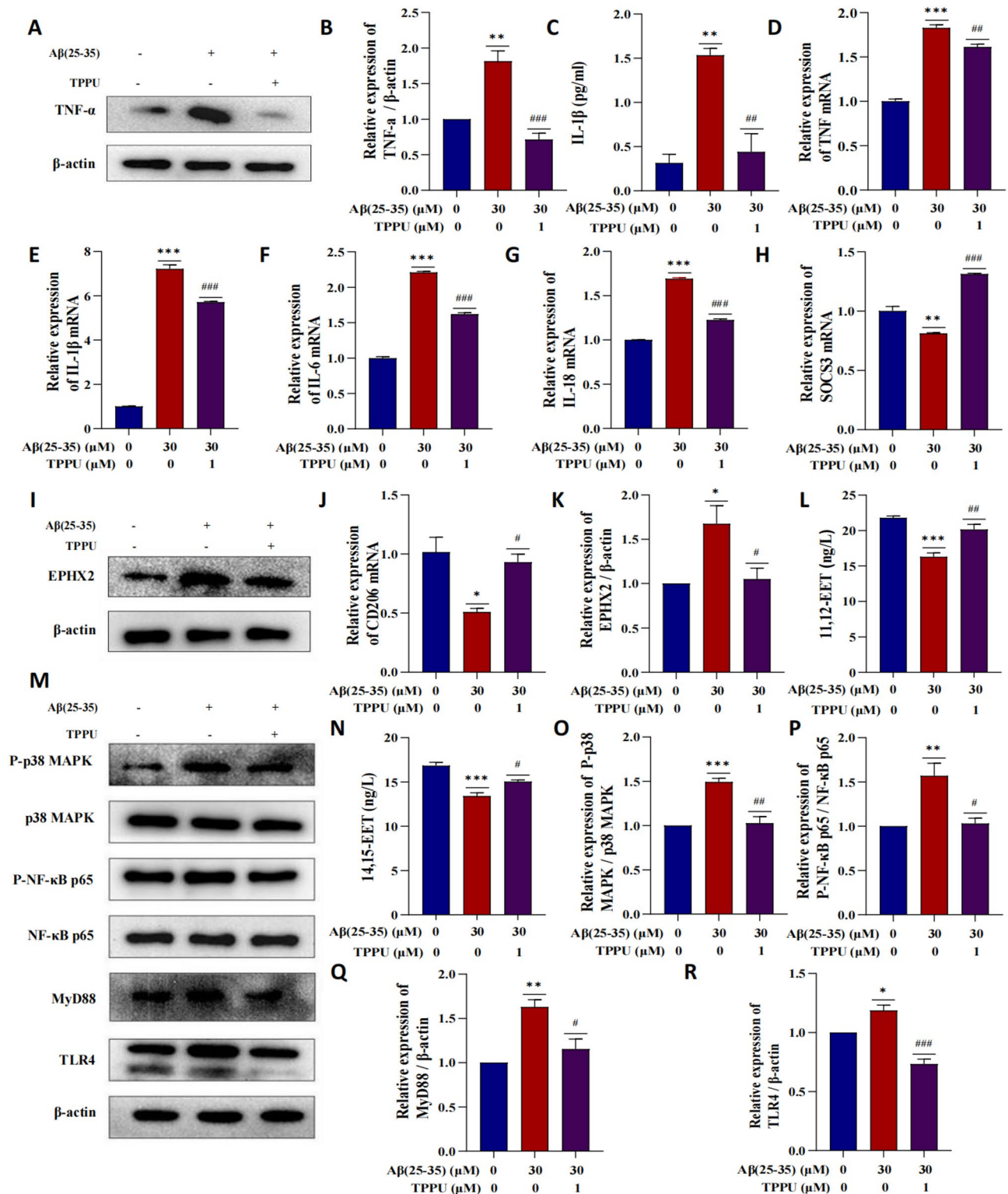


Fig. 5 TPPU against the Aβ(25–35)-induced neuroinflammatory response in HMC3 cells. The expression levels of TNF-α (A, B), EPHX2 (I, K), P-p38 MAPK (M, O), p38 MAPK (M), P-NF-κB p65 (M, P), NF-κB p65 (M), MyD88 (M, Q) and TLR4 (M, R) in HMC3 cells were analyzed by Western Blot. IL-1β (C), 11,12-EET (L) and 14,15-EET (N) levels in cell culture medium were measured by ELISA. The mRNA expression of TNF (D), IL-1β (E), IL-6 (F), IL-18 (G), SOCS3 (H) and CD206 (J) were measured by real-time PCR. The Aβ(25–35) group was compared with the control group, * $P < 0.05$, ** $P < 0.01$ and *** $P < 0.001$; the Aβ(25–35) group was compared with the TPPU pretreatment group, # $P < 0.05$, ## $P < 0.01$ and ### $P < 0.001$. $n = 3$, means \pm SEMs. The data were analyzed using one-way analysis of variance (ANOVA) and Bonferroni post event test

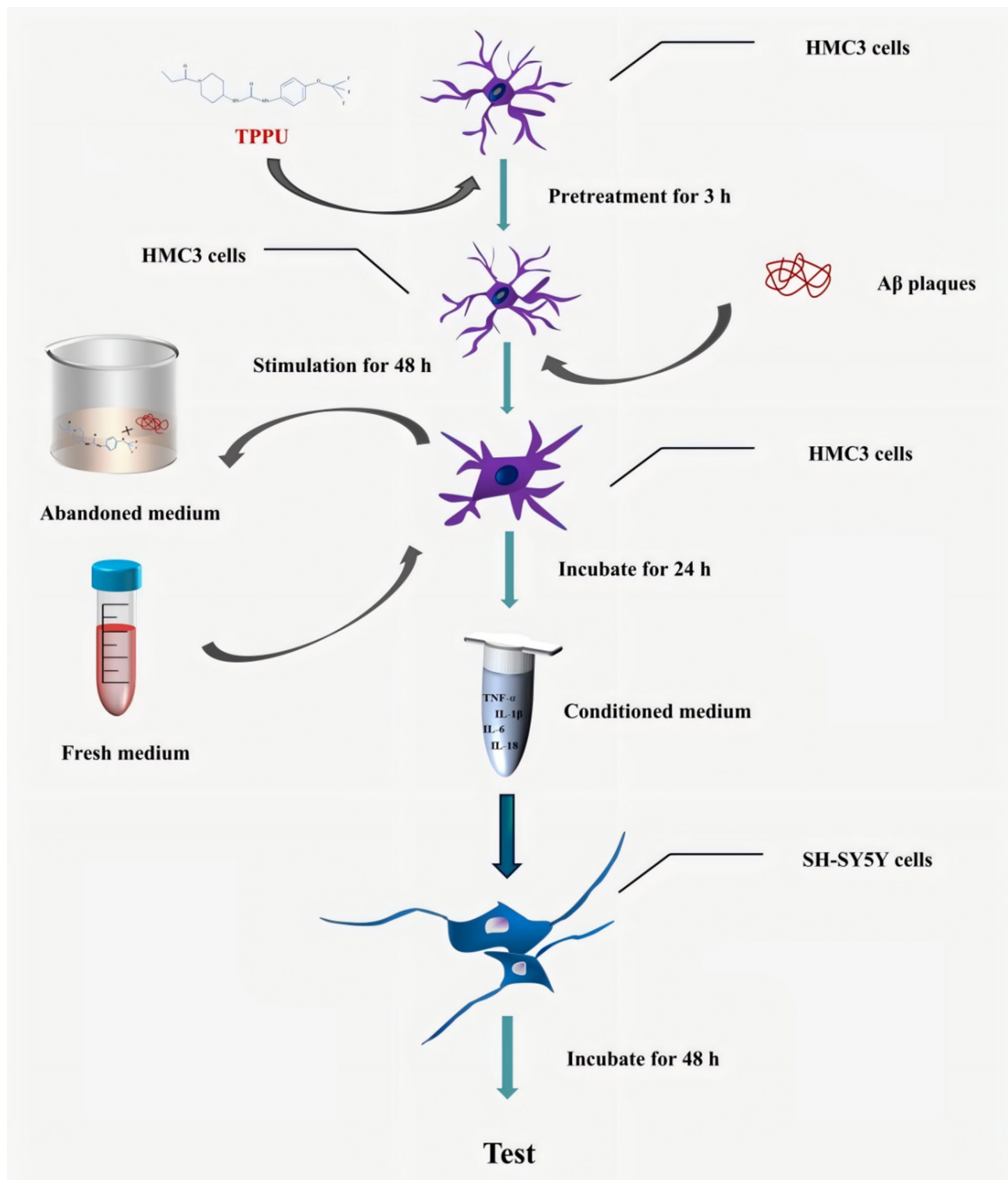


Fig. 6 Schematic diagram of coculturing experiments. HMC3 cells were pretreated with TPPU for 3 h followed by Aβ(25–35) stimulation for an additional 48 h. The medium was replaced with fresh medium and then incubated for 24 h to prepare conditioned medium containing various inflammatory cytokines secreted by HMC3 cells. The collected conditioned medium was centrifuged, added to SH-SY5Y cells, and incubated for 48 h for further analysis

cytokines in microglia [37]. Therefore, we first performed Western Blot to measure the protein levels of TLR4 and MyD88 during the inflammatory process that was mediated by A β (25–35). We found the protein expression of TLR4 and MyD88 was significantly upregulated in the A β group compared with the control group. However, treatment with TPPU effectively reduced the protein levels of TLR4 and MyD88 (Fig. 5M, Q,R). Considering that MyD88 signal transduction mediates the NF- κ B pathway, we used Western Blot to evaluate the effect of TPPU treatment on NF- κ B signal transduction. Of note, neuroinflammation is characterized by the presence of activated microglia and astrocytes surrounding amyloid plaques [38]. A β promotes microglia activation, there by secretes pro-inflammatory cytokines including TNF- α , IL-1 β , IL-6, and IL-18, paralleled through up-regulating NF- κ B activity. As expected, we found that A β (25–35) increased NF- κ B p65 protein phosphorylation, TPPU significantly restrained the activation of microglia, as well as reduced the pro-inflammatory cytokines and NF- κ B activity (Fig. 5M, P). Previous studies have reported that p38 kinase is abnormally active in glial cells in the brains of patients with AD, which increases the expression of inflammatory genes and upregulates proinflammatory cytokines [39]. The protein expression of p38 MAPK and P-p38 MAPK were measured by Western Blot. It was found that A β (25–35) did not change the protein level of p38 MAPK but increased the protein expression of P-p38 MAPK; however, these changes in the protein expression of P-p38 MAPK were reversed after TPPU treatment (Fig. 5M, O). This finding suggested that A β activates the p38 MAPK/NF- κ B pathway to promote neuroinflammation in microglia. In summary, the anti-inflammatory effect of TPPU may be related to the inhibition of the TLR4/MyD88/NF- κ B pathway and p38 MAPK/NF- κ B pathway in microglia.

The neuroprotective and anti-neuroinflammatory effects of TPPU on SH-SY5Y cells cultured with conditioned medium from HMC3 cells

Under physiological conditions, microglia can sense changes in the surrounding environment and maintain the growth and function of neurons. However, under conditions of continuous A β stimulation, microglia release inflammatory cytokines that could cause irreversible damage to neurons [10]. To simulate these pathological conditions, we established neuroglial cocultures to assess the link between neuroprotection and neuroinflammation. First, HMC3 cells were seeded in a 6-well plate. After the cells adhered, the experimental group was treated with 1 μ M TPPU. Because TPPU was dissolved in DMSO, to eliminate the effect of DMSO on the

experimental results, the control group and A β group were treated with medium containing 1 μ M DMSO. Then, after incubation for 3 h, 30 μ M A β (25–35) was added and incubated for 48 h. Then, we collected the culture media from each group and centrifuged these media at 300 \times g for 10 min to remove the pellets; these media were used as conditioned media. SH-SY5Y cells in different groups were cultured in conditioned medium for 48 h. We first performed a CCK-8 assay to evaluate the viability of SH-SY5Y cells after being cultured with conditioned medium from HMC3 cells. Compared with the group that was cultured with control medium, the viability of SH-SY5Y cells that were cultured with medium from the A β group was significantly decreased, while the viability of SH-SY5Y cells that were cultured with medium from the TPPU group was increased (Fig. 7A). Hoechst 33258 fluorescence staining showed that the fluorescence in the nuclei of the control group and the treatment group showed clear and light blue staining, while the nuclei of the A β group were dense and heavily stained (Fig. 7B, E). This indicated that there were more apoptotic cells after culture with medium from the A β group, and TPPU had a neuroprotective effect. It has been reported that neuroinflammation can exacerbate oxidative damage in AD, so we evaluated the changes in ROS in cells that were cultured with different conditioned media. The green fluorescence emitted by the DCFH-DA probe in cells that were cultured with medium from the A β group was much brighter than that in cells that were cultured with medium from the TPPU group (Fig. 7C, H). MDA content (Fig. 7D) as ROS levels increased, while SOD activity decreased (Fig. 7F). TPPU reversed these changes, which further confirmed the neuroprotective effect of TPPU. To investigate the effect of inflammatory cytokines secreted by microglia in neuroglial cocultures on neuronal neuroinflammation, we examined the changes in inflammatory cytokines in SH-SY5Y cells that were cultured in conditioned medium. The protein levels of TNF- α (Fig. 7I, K), and IL-1 β levels (Fig. 7G) produced by SH-SY5Y cells cultured with medium from the A β group were significantly increased compared with those in the group cultured with control medium. Additionally, we used real-time PCR to measure the expression of inflammatory factors, and we found that the mRNA expression levels of IL-1 β , IL-6, and IL-18 were upregulated in SH-SY5Y cells cultured with medium from the A β group (Fig. 7J, L,M). These changes in inflammatory cytokines were reversed in SH-SY5Y cells cultured with medium from the TPPU group. These results indicated that TPPU exerted an anti-neuroinflammatory effect on SH-SY5Y cells exposed to conditioned medium.

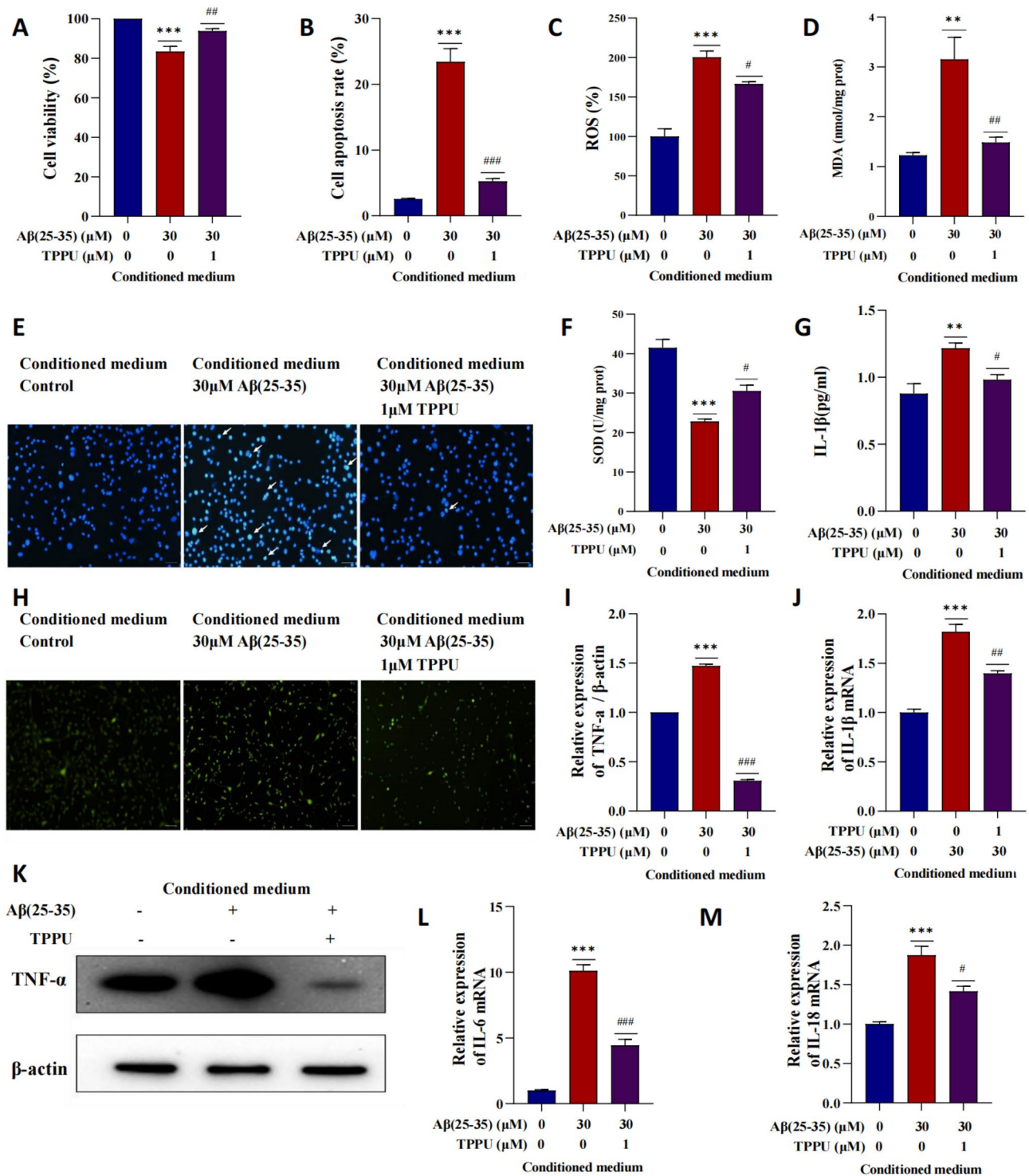


Fig. 7 The neuroprotective and anti-neuroinflammatory effects of TPPU on SH-SY5Y cells cultured with conditioned medium from HMC3 cells. **A** Viability was determined by CCK-8 assay. **B** Apoptotic cells were quantified by Hoechst 33258 staining. **C** Average fluorescence intensity of ROS (normalized to the control group). **D** MDA content. **E** Hoechst 33258 staining; arrows indicate apoptotic cells. Scale bar=100 μm. **F** SOD activity. **G** IL-1β levels in cell culture medium were measured by ELISA. **H** ROS were imaged under a fluorescence microscope. **I**, **K** The expression levels of TNF-α in SH-SY5Y cells cultured with conditioned medium from HMC3 cells was analyzed by Western Blot. The mRNA expression of IL-1β (**J**), IL-6 (**L**), IL-18 (**M**) were measured by real-time PCR. SH-SY5Y cells cultured with medium from the Aβ group were compared with SH-SY5Y cells cultured with control medium, * $P < 0.05$, ** $P < 0.01$ and *** $P < 0.001$; SH-SY5Y cells cultured with medium from the Aβ group were compared with SH-SY5Y cells cultured with medium from the TPPU group, # $P < 0.05$, ## $P < 0.01$ and ### $P < 0.001$. $n = 3$, means \pm SEMs. The data were analyzed using one-way analysis of variance (ANOVA) and Bonferroni post event test

TPPU exerts anti-neuroinflammatory effect by increasing EET levels and its antineuroinflammatory effect on SH-SY5Y cells cultured with conditioned medium from HMC3 cells by regulating the TLR4/NF- κ B and p38 MAPK/NF- κ B signaling pathways

We further examined the protein expression of EPHX2 in SH-SY5Y cells that were cultured in conditioned medium from different groups. We found that the protein expression of EPHX2 was significantly increased in SH-SY5Y cells cultured with medium from the A β group, while the protein expression of EPHX2 was decreased in SH-SY5Y cells cultured with medium from TPPU group (Fig. 8A, B). Furthermore, we found that the levels of 11,12-EET and 14,15-EET were decreased in SH-SY5Y cells cultured with medium from the A β group, while these levels were increased in SH-SY5Y cells cultured with medium from the TPPU group (Fig. 8C, D). This indicates that inhibition of sEH could increase EET levels and alleviate neuroinflammation in AD.

To further explore the mechanism by which TPPU exerts its antineuroinflammatory effect, Western Blot experiments were performed to assess components of the TLR4/NF- κ B pathway and p38 MAPK/NF- κ B pathway in neuroglial coculture. We found that the protein

expression of TLR4, P-NF- κ B p65 and P-p38 MAPK was significantly upregulated in SH-SY5Y cells cultured with medium from the A β group. The protein expression of TLR4, P-NF- κ B p65 and P-p38 MAPK was decreased in SH-SY5Y cells cultured with medium from the TPPU group. The protein expression of NF- κ B p65 and p38 MAPK was not affected in SH-SY5Y cells cultured with medium from the A β group or the TPPU group (Fig. 8E-H). In summary, the anti-inflammatory effect of TPPU may be related to the inhibition of the TLR4/NF- κ B pathway and p38 MAPK/NF- κ B pathway in neuroglial coculture.

Discussion

AD is a degenerative disease of the nervous system that not only causes great suffering for patients but also poses a heavy burden to families and society. As the global population ages, AD will become a worldwide health problem. Research on the mechanism underlying the pathology of AD is ongoing. We hope that we will identify new effective treatments by studying the pathological mechanism of AD. Animal models of AD are important tools for performing basic research to explore the

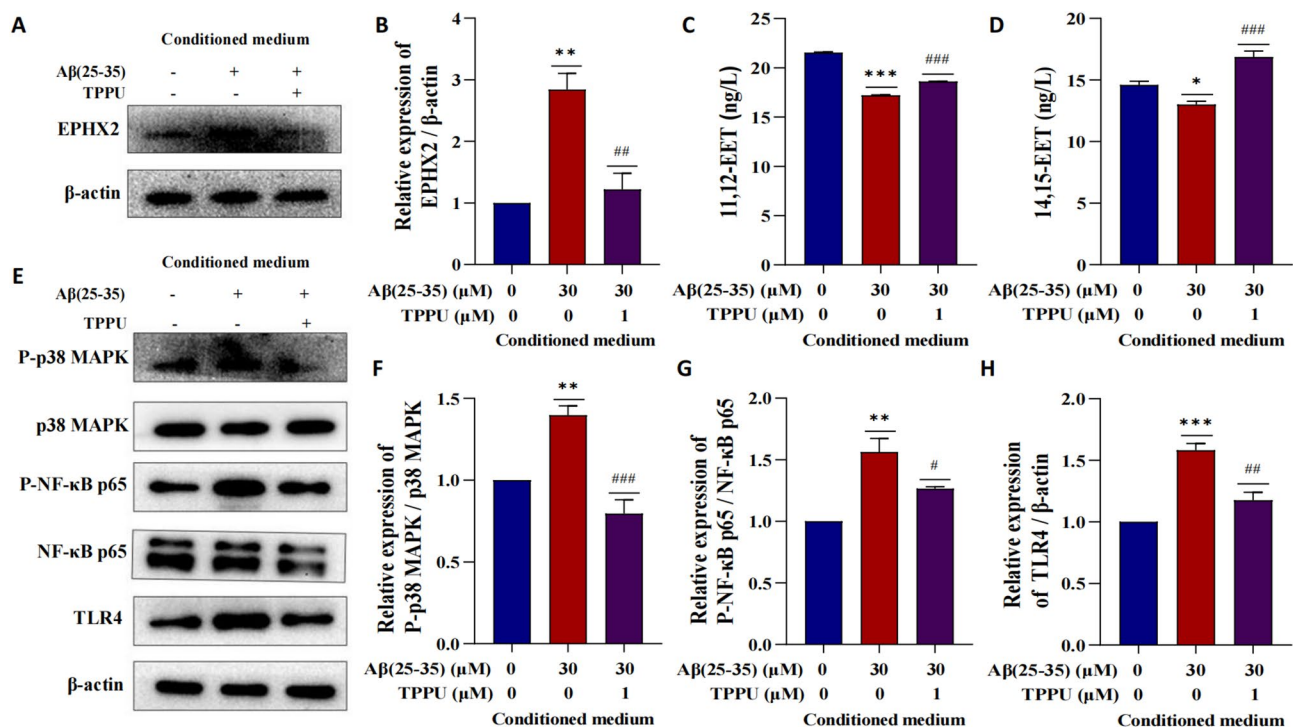


Fig. 8 TPPU exerts an antineuroinflammatory effect by regulating the TLR4/NF- κ B and p38 MAPK/NF- κ B signaling pathways in SH-SY5Y cells cultured with conditioned medium from HMC3 cells. The expression levels of EPHX2 (A, B), P-p38 MAPK (E, F), p38 MAPK (E), P-NF- κ B p65 (E, G), NF- κ B p65 (E), and TLR4 (E, H) in SH-SY5Y cells cultured with conditioned medium from HMC3 cells were analyzed by Western Blot. 11,12-EET (C) and 14,15-EET (D) levels in cell culture medium were measured by ELISA. SH-SY5Y cells cultured with medium from the A β group were compared with SH-SY5Y cells cultured with control medium, * P < 0.05, ** P < 0.01 and *** P < 0.001; SH-SY5Y cells cultured with medium from the A β group were compared with SH-SY5Y cells cultured with medium from the TPPU group, # P < 0.05, ## P < 0.01 and ### P < 0.001. n = 3, means \pm SEMs. The data were analyzed using one-way analysis of variance (ANOVA) and Bonferroni post event test

pathogenesis and treatment of AD as well as for studying new drug development.

EETs are epoxygenated metabolites of C-20 arachidonic acid, and EETs belong to a group of potent chemical mediators termed eicosanoids. Together with prostaglandins and leukotrienes, these eicosanoids have been extensively studied in the mammalian systems in the context of human health and drug development [40, 41]. In recent years, an increasing number of studies have shown that EETs are closely associated with the occurrence and development of AD, and EETs have been proven to exert anti-inflammatory and neuroprotective effects on AD [25]. However, EETs have a very limited function, and they can be rapidly degraded by sEH into the corresponding diol or dihydroxycarbotrienoic acid and lose their activity. sEH is widely expressed in the central nervous system (CNS) [20]. sEH has an N-terminal phosphatase domain and a C-terminal hydrolase domain, and it is encoded by the EPHX2 gene. Elevated expression of sEH has been described in central nervous system diseases such as cerebral hemorrhage [24], depression [42], PD [23], and AD [43]. It was reported that sEH is elevated in the brain tissues of patients with AD, depression, bipolar disorder, schizophrenia, and other diseases after death [23]. There may be a relationship between sEH expression and neuroinflammation. Inhibition of sEH exerts significant anti-inflammatory effects on microglia, astrocytes, and neurons in the central nervous system [27, 44]. The sEH inhibitor application and sEH gene knockout are effective ways to improve the bioavailability of EETs. TPPU is a potent compound (1,3-di-substituted urea) with drug-like properties [28, 45]. Its blood concentration increases in a dose-dependent manner during treatment, and it can enter the brain through the blood-brain barrier [28, 46, 47].

Flies has a high degree of homology with humans at the genetic level, and flies has 548 homologous genes among the 714 known genes that are responsible for human genetic diseases; thus, flies have become an efficient model for research on AD [48]. Flies do not have an integrated blood-brain barrier, such as that observed in humans, and drugs can easily enter the brain of flies, which makes flies an excellent genetic animal model for studying neurodegenerative diseases. In addition, this model has the advantages of low cost, simple feeding methods, short life cycle, strong reproduction ability, large offspring numbers, and ease of phenotype analysis [41, 49, 50]. We used the UAS-GAL4 system to express A β 42 pan-neuronally to investigate the effect of aging on A β 42-expressing flies as well as the anti-neuroinflammatory and neuroprotective effects of TPPU. We found that the cognitive and executive abilities of A β 42-expressing flies were significantly decreased with increasing age, and these observations similar to the clinical manifestations

of human AD [2]. We studied the behavior of A β 42-expressing flies at 14 days and 21 days of age and found that as the age of A β 42 flies increased, the toxic effects of A β increased, lifespan decreased, and crawling ability and olfactory memory were reduced. The ability of A β 42 flies to resist oxidative damage was decreased at 21 days of age compared to that of A β 42 flies at 14 days of age.

To our knowledge, no study has been conducted on the effect of TPPU on the AD flies model. We investigated whether TPPU exerts a neuroprotective effect against A β toxicity in A β 42-transgenic flies. We found that TPPU could improve the behavioral performance of A β 42-transgenic flies. TPPU prolonged the survival time of A β 42-transgenic flies. TPPU improved the crawling ability and olfactory memory of 14-day-old and 21-day-old A β 42-transgenic flies, suggesting that TPPU exerts a neuroprotective effect against A β toxicity. In the following experiments, we measured MDA content and SOD activity, and we found that TPPU could decrease the MDA content and increase the SOD activity in the brain tissues of A β 42-transgenic flies, which indicated that TPPU could protect against peroxidation and oxidative damage.

In mammals, EETs are short-lived lipid signaling molecules, and are mainly hydrolyzed by sEH, which was discovered while studying the mammalian metabolism of insect juvenile hormone and its analogs [51]. The sEH turned out to be a therapeutic target for a variety of mammalian diseases [52–54]. In insects, epoxide hydrolases with activities on juvenile hormones (JHEHs) are the best characterized epoxide hydrolases (EHs) [55, 56]. These JHEHs are believed to be involved in the metabolic degradation of juvenile hormones in vivo, which are key developmental and reproductive hormones [57, 58]. So far, the insect microsomal epoxide hydrolase (mEHs) and JHEHs characterized are homologous to mammalian microsomal epoxide hydrolases [19, 59]. The *Anopheles gambiae* characterized here shows evolutionary, biochemical, and immunological similarities to mammalian sEH, suggesting there are sEH homologs in insects, and epoxy fatty acids may be important chemical mediators for insects [58]. In a study, sEH inhibitors 1-[(1-Acetylpiperidin-4-yl)-3-adamantan-1-yl]urea (APAU) was evaluated for their antiparkinsonian activity against rotenone (ROT) induced neurodegeneration in *Drosophila melanogaster* model of PD. They found that APAU significantly attenuates ROT induced changes in survival rate, negative geotaxis, oxidative stress, dopamine and its metabolites levels in *Drosophila melanogaster* model of PD [30]. Regrettably, it is not known whether insect epoxide hydrolases play other important roles in insect physiology, and what other substrates can be involved.

Previous studies found that the level of sEH was increased in the brain tissues of APP/PS1 Tg mice, mainly

in hippocampal astrocytes. sEH gene knockout reduced A β plaque deposition, improved behavior and delayed the progression of AD in APP/PS1 Tg mice. In addition, inhibition of sEH function increased astrocyte hyperplasia and the levels of astrocyte-derived anti-inflammatory cytokines, including IL-4 and IL-10, as well as the activity of NF- κ B and nuclear factor of activated T cells (NFAT) in APP/PS1 Tg mice [27]. Cheng-Peng Sun et al. found that the expression and activity of sEH in the hippocampus were significantly increased in an A β -induced AD mouse model. The selective sEH inhibitor TPPU chemically inhibits sEH, which can alleviate spatial learning and memory deficits and elevate neurotransmitter levels in A β -induced AD model mice. In addition, inhibition of sEH could alleviate neuroinflammation, neuronal death and oxidative stress by stabilizing the levels of EETs, particularly 8,9-epoxyeicosatrienoic acid (8,9-EET) and 14,15-EET, in vivo [60, 61]. Although previous studies showed that inhibiting sEH activity could alleviate neuroinflammatory responses [26], it is unclear how the sEH inhibitor exerts its anti-neuroinflammatory effects in cocultures of neuronal cells, microglia, and neuroglia. In this study, we established in vitro cell models to simulate the pathological effects of A β on neurons, microglia, and neuroglia in coculture systems, and we further explored the neuroprotective and anti-neuroinflammatory effects of the sEH inhibitor TPPU. The most notable feature of AD patients is the progressive decline in cognitive ability, which mainly occurs due to the loss of neurons and synapses in the hippocampus and related brain areas [2]. We used A β (25–35)-stimulated SH-SY5Y cells to model the neuronal destruction caused by A β in the pathogenesis of AD and then studied whether TPPU could exert neuroprotective and antineuroinflammatory effects against A β toxicity. In this experiment, we found that TPPU could improve the viability of SH-SY5Y cells treated with A β (25–35), alleviate damage to cell axons, increase the number of cells, and decrease ROS production and apoptosis. In addition, TPPU can inhibit lipid peroxidation and oxidative damage by decreasing MDA content and increasing SOD activity. More importantly, TPPU can alleviate the inflammatory response of SH-SY5Y cells stimulated by A β (25–35). These neuroprotective and antineuroinflammatory effects were closely related to the stabilization of EET levels, and TPPU inhibited the protein expression of the sEH-encoding gene EPHX2 and increased the 11,12-EET and 14,15-EET levels.

Microglia play a dual role in the pathogenesis of AD. On the one hand, activated microglia produce anti-inflammatory cytokines, such as IL-4 and IL-10, to reduce the inflammatory response in the brain tissues of AD patients and generate anti-A β antibodies to clear the amyloid plaques that are deposited in the brain tissues, alleviating the degeneration associated with AD [62]. On

the other hand, when microglia are overactivated, they release toxic substances, such as ROS and NO, and pro-inflammatory cytokines, such as IL-1, IL-6, and TNF- α , which lead to an increase in oxidative stress and chronic inflammation in the brain, indirectly triggering neuronal dysfunction and a reduction in synaptic plasticity, leading to neuronal damage and degeneration, and ultimately destroying neurons. Studies have shown that the levels of inflammatory cytokines in microglia of AD patients was 30 times greater than that of the control group [63], and the increased inflammatory cytokines inhibited phagocytosis of microglia, weakened the ability to clear A β , led to A β deposition, and further exacerbated AD [12]. In this experiment, we further investigated the effect of TPPU on HMC3 cells treated with A β (25–35). We found that TPPU increased cell viability, reduced oxidative stress in HMC3 cells that were treated with A β (25–35). Furthermore, we measured the 11,12-EET and 14,15-EET levels in cells by ELISA and found that both were decreased in HMC3 cells treated with A β (25–35). After TPPU treatment, the 11,12-EET and 14,15-EET levels were increased in HMC3 cells treated with A β (25–35). Subsequently, we measured EPHX2 protein expression by Western Blot and found that the EPHX2 protein level was increased in HMC3 cells treated with A β (25–35) and decreased after TPPU treatment. It was confirmed that TPPU played a neuroprotective role by inhibiting sEH and increasing EET levels. Can TPPU alleviate microglia-induced neuroinflammation? We measured the production of inflammatory cytokines by microglia by ELISA, Western Blot, and real-time PCR, and we found that TPPU inhibited the expression of proinflammatory cytokines in HMC3 cells treated with A β (25–35). TPPU decreased the IL-1 β levels in the culture medium of HMC3 cells treated with A β (25–35) and decreased the protein expression level of TNF- α and the mRNA expression levels of TNF, IL-1 β , IL-6 and IL-18 in HMC3 cells treated with A β (25–35). This observation suggests that TPPU could mitigate the M1 polarization of microglia. In addition, we found that the mRNA expression levels of the anti-inflammatory phenotypic markers CD206 and SOCS3 were increased after TPPU treatment, which suggests that TPPU could promote the polarization of microglia toward the M2 type. It was confirmed that TPPU could alleviate microglia-induced neuroinflammation. Glia-neuron interactions are key to AD pathology. Proinflammatory cytokines released by microglia not only cause direct toxicity to neurons but also exacerbate A β plaque formation, which leads to a vicious cycle between AD pathology and neuroinflammation [11]. To our knowledge, there have been no reports on the effect of TPPU on neuroglial coculture. In the neuroglial coculture, the inflammatory cytokines released by microglia after A β stimulation reduced the viability of SH-SY5Y

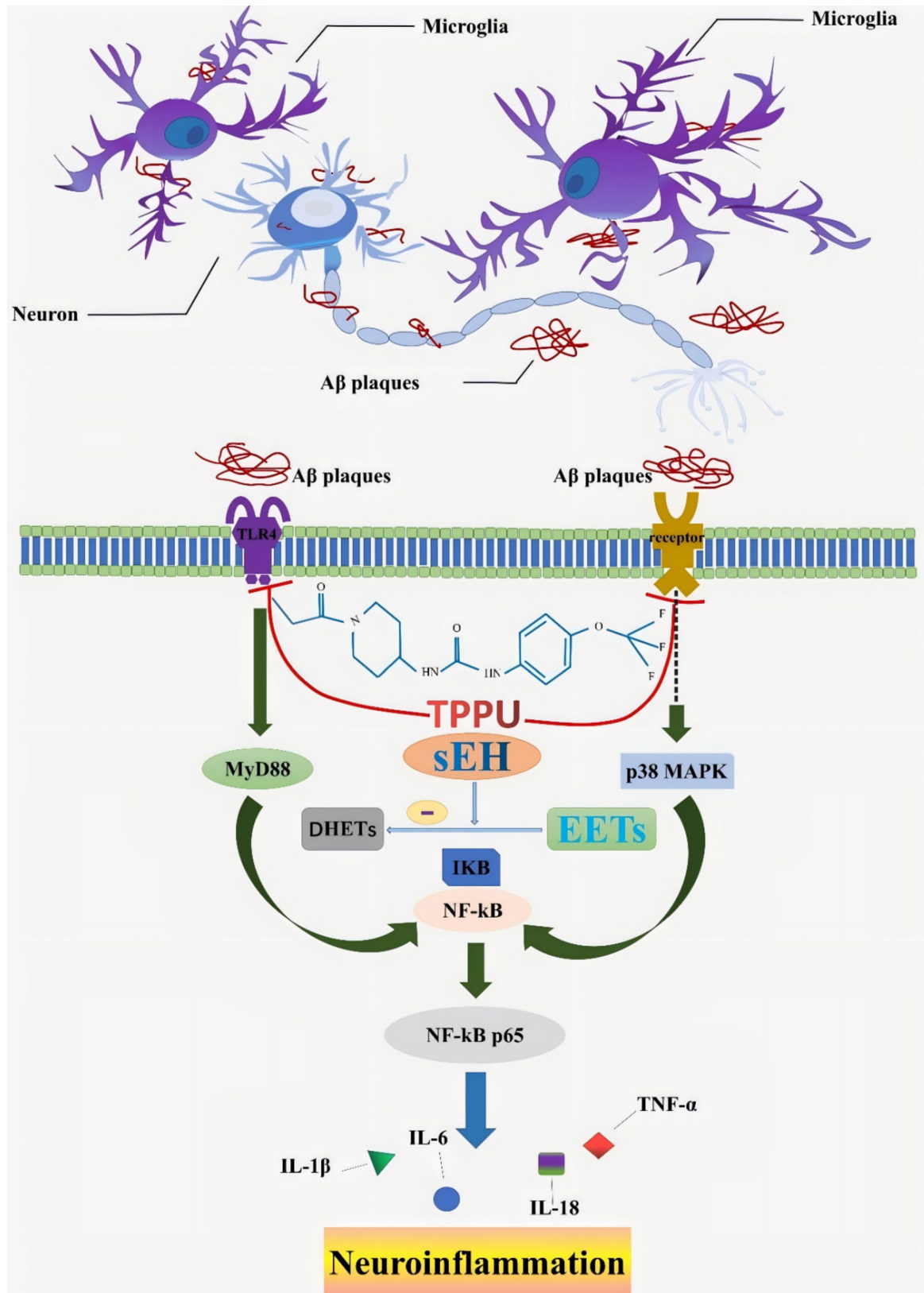


Fig. 9 Potential mechanism underlying the protective effect of TPPU against neuroinflammation in Alzheimer's disease

cells, increased apoptosis, aggravated oxidative damage, and upregulated the levels of the inflammatory cytokines TNF- α , IL-1 β , IL-6, and IL-18. Furthermore, we found that TPPU could reverse these changes, that the 11,12-EET and 14,15-EET levels in the TPPU group were higher than those in the A β group in the glial coculture system, and that the protein expression of EPHX2 was decreased, which verified that the sEH inhibitor could enhance neuroprotective and anti-inflammatory effects by stabilizing endogenous EETs.

TLR4 is expressed in neurons, microglia, astrocytes, and oligodendrocytes of the central nervous system and can be activated by many cytokines [64]. TLR4 mainly activates the NF- κ B signaling pathway. NF- κ B, a member of the transcription factor Rel family, is ubiquitous in the cytoplasm, is a component of the signaling pathway downstream of TLR4, and has been shown to be involved in the regulation of neuroinflammation [65]. Under normal conditions, NF- κ B p65, NF- κ B p50, and the inhibitory protein I κ B bind together, which maintains NF- κ B in the inactive state. A β can activate NF- κ B in glial and neuronal cells. When cells are stimulated by A β , IKK is activated, I κ B is phosphorylated and subsequently ubiquitinated and degraded, and then NF- κ B is released and transported to the nucleus. After activation of the TLR4/NF- κ B signaling pathway, NF- κ B can regulate the expression of inflammatory cytokines, such as IL-1 β , IL-6, and TNF- α . These inflammatory cytokines can regulate the TLR4/NF- κ B signaling pathway; thus, they form a feedback loop and participate in the pathological process of neuroinflammation [66]. We found that TPPU treatment downregulated the expression of TLR4 and P-NF- κ B p65 in SH-SY5Y and HMC3 cells cocultured with A β (25–35) and neuroglia. These results suggest that TPPU exerts antineuroinflammatory effects by inhibiting the activation of the TLR4/NF- κ B signaling pathway. In the future, we will further study the degradation of I κ B downstream.

p38 MAPK is a key regulator of various cellular stress responses. Previous studies have shown that the levels of phosphorylated p38 are increased in the brains of patients [39]. A recent clinical study reported that increased levels of phosphorylated p38 MAPK in blood were related to the severity of AD [67]. p38 MAPK plays a crucial role in activating microglial intracellular signal transduction and in the neuronal response to glia-derived neurotoxic molecules [68, 69]. p38 MAPK is the most important regulator of A β -induced toxicity. p38 can induce NF- κ B activation, promote glutamate excitotoxicity and disrupt synaptic plasticity, and it can regulate the expression of proinflammatory cytokines and inflammatory genes, finally triggering neuroinflammation. These results prove that p38 MAPK is a potential target for disrupting the vicious cycle of A β toxicity [69]. In our study, we found that TPPU could inhibit the increase in P-p38

MAPK levels stimulated by A β (25–35) in cocultures of nerve cells, microglia, and neuroglia, which suggested that TPPU could exert its anti-neuroinflammatory effect by inhibiting the p38 MAPK/NF- κ B pathway. In summary, TPPU can reduce neuroinflammation by inhibiting the TLR4/NF- κ B pathway and p38 MAPK/NF- κ B pathway in AD cell models. (Fig. 9).

Conclusion

In conclusion, we found that the sEH inhibitor TPPU exerts neuroprotective and anti-neuroinflammatory effects in AD models. In vivo, we found that TPPU could significantly improve behavioral performance and decrease oxidative damage in A β 42-transgenic flies. In vitro experiments, we found that inhibition of sEH could stabilize the level of EETs (11,12-EET and 14,15-EET), and TPPU could reduce neuroinflammation by inhibiting TLR4/NF- κ B and p38 MAPK/NF- κ B pathway activation in AD cell models. These findings provide new insights into the pathogenesis of neuroinflammation in AD and reveal new therapeutic targets for AD.

Abbreviations

AD	Alzheimer's disease
EETs	Epoxyeicosatrienoic acids
sEH	Soluble epoxide hydrolase
TPPU	1-Trifluoromethoxyphenyl-3-(1-propionylpiperidin-4-yl) urea
8,9-EET	8,9-epoxyeicosatrienoic acid
11,12-EET	11,12-epoxyeicosatrienoic acid
14,15-EET	14,15-epoxyeicosatrienoic acid
GAL4	Galactose-regulated upstream promoter element 4
UAS	Upstream active sequence
MDA	Malondialdehyde
SOD	Superoxide dismutase
ROS	Reactive oxygen species
TNF- α	Tumor necrosis factor- α
IL-1 β	Interleukin-1 β
TLR4	Toll Like Receptor 4
MAPK	Mitogen activated protein kinases

Acknowledgements

We thank the State Key Laboratory of Medical Genetics, Central South University for generously giving us flies (whole neuronal expression of elavb red/GAL4).

Authors' contributions

Conception or design: Xiaowen Sun, Jixu Yu, Bruce D Hammock, Hongxiang Liu. Acquisition, analysis, or interpretation of data: Xiaowen Sun, Hongxiang Liu, Wei Li, Lin Li, Qian Tian, Qingyang Cao, Yun Meng, Yan Shen, Fengyuan Che, Joanna C Chiu, Jixu Yu, Bruce D Hammock. Drafting the work or revising: Xiaowen Sun, Yun Meng, Wei Li. Final approval of the manuscript: Xiaowen Sun, Jixu Yu, Bruce D Hammock. All authors reviewed the manuscript.

Funding

This work was supported by a grant from Linyi Science and Technology Development Program, China (201919010).

Data availability

No datasets were generated or analysed during the current study.

Declarations

Consent for publication

All listed authors consent to the submission.

Competing interests

The authors declare no competing interests.

Author details

¹Department of Neurology, Linyi People's Hospital, Linyi 276000, Shandong, China

²Shandong Provincial Clinical Research Center for Geriatric Diseases, Linyi 276000, Shandong, China

³Department of Entomology and Nematology, College of Agricultural and Environmental Sciences, University of California Davis, Davis, CA 95616, USA

⁴Department of Entomology and Nematology and UCD Comprehensive Cancer Center, University of California, Davis, CA 95616, USA

Received: 4 March 2025 / Accepted: 29 May 2025

Published online: 23 June 2025

References

- Serrano-Pozo A, Frosch MP, Masliah E, Hyman BT. Neuropathological alterations in alzheimer disease. *Cold Spring Harbor Perspect Med*. 2011;1:a006189.
- Scheltens P, De Strooper B, Kivipelto M, Holstege H, Chételat G, Teunissen CE, et al. Alzheimer's disease. *Lancet (London England)*. 2021;397:10284:1577–90.
- Estimation of the global prevalence of dementia. In 2019 and forecasted prevalence in 2050: an analysis for the global burden of disease study 2019. *Lancet Public Health*. 2022;7(2):e105–25.
- Ferrari C, Sorbi S. The complexity of alzheimer's disease: an evolving puzzle. *Physiol Rev*. 2021;101(3):1047–81.
- Tatullian SA. Challenges and hopes for alzheimer's disease. *Drug Discovery Today*. 2022;27(4):1027–43.
- Cummings J, Lee G, Nahed P, Kamar M, Zhong K, Fonseca J, et al. Alzheimer's disease drug development pipeline: 2022. *Alzheimers Dement (New York, N Y)*. 2022;8(1):e12295.
- Du X, Wang X, Geng M. Alzheimer's disease hypothesis and related therapies. *Translational Neurodegeneration*. 2018;7:2.
- Calsolaro V, Edison P. Neuroinflammation in alzheimer's disease: current evidence and future directions. *Alzheimer's Dement J Alzheimer's Assoc*. 2016;12(6):719–32.
- Cheng J, Dong Y, Ma J, Pan R, Liao Y, Kong X et al. Microglial Calhm2 regulates neuroinflammation and contributes to Alzheimer's disease pathology. *Sci Adv*. 2021;7:eabe3600.
- Leng F, Edison P. Neuroinflammation and microglial activation in alzheimer disease: where do we go from here? *Nat Reviews Neurol*. 2021;17(3):157–72.
- Cai Y, Liu J, Wang B, Sun M, Yang H. Microglia in the neuroinflammatory pathogenesis of alzheimer's disease and related therapeutic targets. *Front Immunol*. 2022;13:856376.
- Hansen DV, Hanson JE, Sheng M. Microglia in alzheimer's disease. *J Cell Biol*. 2018;217(2):459–72.
- Al-Ghraiyyah NF, Wang J, Alkhalifa AE, Roberts AB, Raj R, Yang E, et al. Glial Cell-Mediated Neuroinflammation in Alzheimer's Disease. *Int J Mol Sci*. 2022;23:10572.
- Piccioni G, Mango D, Saidi A, Corbo M, Nisticò R. Targeting Microglia-Synapse Interactions in Alzheimer's Disease. *Int J Mol Sci*. 2021;22:2342.
- Cai Z, Hussain MD, Yan LJ. Microglia, neuroinflammation, and beta-amyloid protein in alzheimer's disease. *Int J Neurosci*. 2014;124(5):307–21.
- Ding Y, Tu P, Chen Y, Huang Y, Pan X, Chen W. CYP2J2 and EETs protect against pulmonary arterial hypertension with lung ischemia-reperfusion injury in vivo and in vitro. *Respir Res*. 2021;22:1291.
- Iliff JJ, Jia J, Nelson J, Goyagi T, Klaus J, Alkayed NJ. Epoxyeicosanoid signaling in CNS function and disease. *Prostaglandins Other Lipid Mediat*. 2010;91(3):4:68–84.
- Ostermann AI, Herbers J, Willenberg I, Chen R, Hwang SH, Greite R et al. Oral treatment of rodents with soluble epoxide hydrolase inhibitor 1-(1-propanoylpiperidin-4-yl)-3-[4-(trifluoromethoxy)phenyl]urea (TPPU): Resulting drug levels and modulation of oxylipin pattern. *Prostaglandins & other lipid mediators*. 2015;121Pt A:131–137.
- Newman JW, Morisseau C, Hammock BD. Epoxide hydrolases: their roles and interactions with lipid metabolism. *Prog Lipid Res*. 2005;44(1):1–51.
- Sura P, Sura R, Enayetallah AE, Grant DF. Distribution and expression of soluble epoxide hydrolase in human brain. *J Histochem Cytochemistry: Official J Histochem Soc*. 2008;56(6):551–9.
- Kodani SD, Morisseau C. Role of epoxy-fatty acids and epoxide hydrolases in the pathology of neuro-inflammation. *Biochimie*. 2019;159:59–65.
- Qin X, Wu Q, Lin L, Sun A, Liu S, Li X, et al. Soluble epoxide hydrolase deficiency or Inhibition attenuates MPTP-Induced parkinsonism. *Mol Neurobiol*. 2015;52(1):187–95.
- Ren Q, Ma M, Yang J, Nonaka R, Yamaguchi A, Ishikawa KI, et al. Soluble epoxide hydrolase plays a key role in the pathogenesis of parkinson's disease. *Proc Natl Acad Sci USA*. 2018;115(25):E5815–23.
- Wu CH, Shyue SK, Hung TH, Wen S, Lin CC, Chang CF, et al. Genetic deletion or Pharmacological Inhibition of soluble epoxide hydrolase reduces brain damage and attenuates neuroinflammation after intracerebral hemorrhage. *J Neuroinflamm*. 2017;14(1):230.
- Chen W, Wang M, Zhu M, Xiong W, Qin X, Zhu X. 14,15-Epoxyeicosatrienoic acid alleviates pathology in a mouse model of alzheimer's disease. *J Neuroscience: Official J Soc Neurosci*. 2020;40(2):8188–203.
- Ghosh A, Comerota MM, Wan D, Chen F, Propson NE, Hwang SH, et al. An epoxide hydrolase inhibitor reduces neuroinflammation in a mouse model of Alzheimer's disease. *Sci Transl Med*. 2020;12:eabb1206.
- Lee HT, Lee KI, Chen CH, Lee TS. Genetic deletion of soluble epoxide hydrolase delays the progression of alzheimer's disease. *J Neuroinflamm*. 2019;16(1):267.
- Ulu A, Appt S, Morisseau C, Hwang SH, Jones PD, Rose TE, et al. Pharmacokinetics and in vivo potency of soluble epoxide hydrolase inhibitors in cynomolgus monkeys. *Br J Pharmacol*. 2012;165(5):1401–12.
- Siddique YH, Rahul, Ara G, Afzal M, Varshney H, Gaur K, et al. Beneficial effects of apigenin on the Transgenic Drosophila model of alzheimer's disease. *Chemico-Biol Interact*. 2022;366:110120.
- Lakkappa N, Krishnamurthy PT, M DP, Hammock BD, Hwang SH. Soluble epoxide hydrolase inhibitor, APAU, protects dopaminergic neurons against rotenone induced neurotoxicity: implications for parkinson's disease. *Neurotoxicology*. 2019;70:135–45.
- Liu Ying L, Liu G. Effects of polygala tenuifolia saponins on behavior and life span of Tau Transgenic Drosophila model of alzheimer's disease. *Jilin Traditional Chin Med*. 2021;41:234–7.
- Balendra V, Singh SK. Therapeutic potential of Astaxanthin and superoxide dismutase in alzheimer's disease. *Open Biology*. 2021;11(6):210013.
- Ionescu-Tucker A, Cotman CW. Emerging roles of oxidative stress in brain aging and alzheimer's disease. *Neurobiol Aging*. 2021;107:86–95.
- De Schepper S, Crowley G, Hong S. Understanding microglial diversity and implications for neuronal function in health and disease. *Dev Neurobiol*. 2021;81(5):507–23.
- Tang Y, Le W. Differential roles of M1 and M2 microglia in neurodegenerative diseases. *Mol Neurobiol*. 2016;53(2):1181–94.
- Gambuzza ME, Sofo V, Salmeri FM, Soraci L, Marino S, Bramanti P. Toll-like receptors in alzheimer's disease: a therapeutic perspective. *CNS Neurol Disord Drug Target*. 2014;13(9):1542–58.
- Leitner GR, Wenzel TJ, Marshall N, Gates EJ, Klegeris A. Targeting toll-like receptor 4 to modulate neuroinflammation in central nervous system disorders. *Expert Opin Ther Targets*. 2019;23(10):865–82.
- Lewcock JW, Schlepckow K, Di Paolo G, Tahirovic S, Monroe KM, Haass C. Emerging microglia biology defines novel therapeutic approaches for alzheimer's disease. *Neuron*. 2020;108(5):801–21.
- Hensley K, Floyd RA, Zheng NY, Nael R, Robinson KA, Nguyen X, et al. p38 kinase is activated in the alzheimer's disease brain. *J Neurochem*. 1999;72(5):2053–8.
- Morisseau C, Hammock BD. Impact of soluble epoxide hydrolase and epoxyeicosanoids on human health. *Annu Rev Pharmacol Toxicol*. 2013;53:37–58.
- Tapiero H, Ba GN, Couvreur P, Tew KD. Polyunsaturated fatty acids (PUFA) and eicosanoids in human health and pathologies. *Biomed pharmacotherapy = Biomedecine Pharmacotherapie*. 2002;56(5):215–22.
- Wu Q, Cai H, Song J, Chang Q. The effects of sEH inhibitor on depression-like behavior and neurogenesis in male mice. *J Neurosci Res*. 2017;95(12):2483–92.
- Griñán-Ferré C, Codony S, Pujol E, Yang J, Leiva R, Escolano C, et al. Pharmacological Inhibition of soluble epoxide hydrolase as a new therapy for alzheimer's disease. *Neurother: J Am Soc Experimental Neurother*. 2020;17(4):1825–35.
- Wang J, Fujiyoshi T, Kosaka Y, Raybuck JD, Lattal KM, Ikeda M, et al. Inhibition of soluble epoxide hydrolase after cardiac arrest/cardiopulmonary resuscitation induces a neuroprotective phenotype in activated microglia and improves neuronal survival. *J Cereb Blood Flow Metab*. 2013;33(10):1574–81.

45. Tsai HJ, Hwang SH, Morisseau C, Yang J, Jones PD, Kasagami T, et al. Pharmacokinetic screening of soluble epoxide hydrolase inhibitors in dogs. *Eur J Pharm Sci.* 2010;403:222–38.
46. Liu JY, Tsai HJ, Hwang SH, Jones PD, Morisseau C, Hammock BD. Pharmacokinetic optimization of four soluble epoxide hydrolase inhibitors for use in a murine model of inflammation. *Br J Pharmacol.* 2009;156:284–96.
47. Wan D, Yang J, McReynolds CB, Barnych B, Wagner KM, Morisseau C, et al. In vitro and in vivo metabolism of a potent inhibitor of soluble epoxide hydrolase, 1-(1-Propionylpiperidin-4-yl)-3-(4-(trifluoromethoxy)phenyl)urea. *Front Pharmacol.* 2019;10:464.
48. Lakkappa N, Krishnamurthy PT, Yamjala K, Hwang SH, Hammock BD, Babu B. Evaluation of antiparkinson activity of PTUPB by measuring dopamine and its metabolites in *Drosophila melanogaster*: LC-MS/MS method development. *J Pharm Biomed Anal.* 2018;149:457–64.
49. Reiter LT, Potocki L, Chien S, Gribskov M, Bier E. A systematic analysis of human disease-associated gene sequences in *Drosophila melanogaster*. *Genome Res.* 2001;11:1114–25.
50. Cheng X, Song C, Du Y, Gaur U, Yang M. Pharmacological Treatment of Alzheimer's Disease: Insights from *Drosophila melanogaster*. *Int J Mol Sci.* 2020;21:4621.
51. Gill SS, Hammock BD, Casida JE. Mammalian metabolism and environmental degradation of the juvenoid 1-(4'-ethylphenoxy)-3,7-dimethyl-6,7-epoxy-trans-2-octene and related compounds. *J Agric Food Chem.* 1974;22:386–95.
52. Imig JD. Epoxide hydrolase and epoxygenase metabolites as therapeutic targets for renal diseases. *Am J Physiol Ren Physiol.* 2005;289:496–503.
53. Imig JD, Hammock BD. Soluble epoxide hydrolase as a therapeutic target for cardiovascular diseases. *Nat Rev Drug Discovery.* 2009;8:794–805.
54. Zhang W, Koerner IP, Noppens R, Grafe M, Tsai HJ, Morisseau C, et al. Soluble epoxide hydrolase: a novel therapeutic target in stroke. *J Cereb Blood Flow Metab.* 2007;27:1931–40.
55. Anspaugh DD, Roe RM. Regulation of JH epoxide hydrolase versus JH esterase activity in the cabbage looper, *Trichoplusia ni*, by juvenile hormone and xenobiotics. *J Insect Physiol.* 2005;51:523–35.
56. Seino A, Ogura T, Tsubota T, Shimomura M, Nakakura T, Tan A, et al. Characterization of juvenile hormone epoxide hydrolase and related genes in the larval development of the silkworm *Bombyx mori*. *Biosci Biotechnol Biochem.* 2010;74:1421–9.
57. Prestwich GD, Wojtasek H, Lentz AJ, Rabinovich JM. Biochemistry of proteins that bind and metabolize juvenile hormones. *Arch Insect Biochem Physiol.* 1996;32:4407–19.
58. Xu J, Morisseau C, Hammock BD. Expression and characterization of an epoxide hydrolase from *Anopheles gambiae* with high activity on epoxy fatty acids. *Insect Biochem Mol Biol.* 2014;54:42–52.
59. Xu J, Morisseau C, Yang J, Mamatha DM, Hammock BD. Epoxide hydrolase activities and epoxy fatty acids in the mosquito *Culex quinquefasciatus*. *Insect Biochem Mol Biol.* 2015;59:41–9.
60. Sun CP, Zhang XY, Zhou JJ, Huo XK, Yu ZL, Morisseau C, et al. Inhibition of sEH via stabilizing the level of EETs alleviated alzheimer's disease through GSK3 β signaling pathway. *Food Chem Toxicology: Int J Published Br Industrial Biol Res Association.* 2021;156:112516.
61. Lauretti E, Dincer O, Praticò D. Glycogen synthase kinase-3 signaling in alzheimer's disease. *Biochim Et Biophys Acta Mol Cell Res.* 2020;1867:118664.
62. Venigalla M, Sonogo S, Gyengesi E, Sharman MJ, Münch G. Novel promising therapeutics against chronic neuroinflammation and neurodegeneration in alzheimer's disease. *Neurochem Int.* 2016;95:63–74.
63. Ng A, Tam WW, Zhang MW, Ho CS, Husain SF, McIntyre RS, et al. IL-1 β , IL-6, TNF- α and CRP in elderly patients with depression or alzheimer's disease: systematic review and Meta-Analysis. *Sci Rep.* 2018;8:12050.
64. Vaure C, Liu Y. A comparative review of toll-like receptor 4 expression and functionality in different animal species. *Front Immunol.* 2014;5:316.
65. Sun E, Motolani A, Campos L, Lu T. The Pivotal Role of NF- κ B in the Pathogenesis and Therapeutics of Alzheimer's Disease. *Int J Mol Sci.* 2022;23:8972.
66. Seo EJ, Fischer N, Efferth T. Phytochemicals as inhibitors of NF- κ B for treatment of alzheimer's disease. *Pharmacol Res.* 2018;129:262–73.
67. Wang S, Zhang C, Sheng X, Zhang X, Wang B, Zhang G. Peripheral expression of MAPK pathways in alzheimer's and parkinson's diseases. *J Clin Neuroscience: Official J Neurosurgical Soc Australasia.* 2014;21:810–4.
68. Lin H, Dixon SG, Hu W, Hamlett ED, Jin J, Ergul A, et al. p38 MAPK is a major regulator of amyloid Beta-Induced IL-6 expression in human microglia. *Mol Neurobiol.* 2022;59:5284–98.
69. Kheiri G, Dolatshahi M, Rahmani F, Rezaei N. Role of p38/MAPKs in alzheimer's disease: implications for amyloid beta toxicity targeted therapy. *Rev Neurosci.* 2018;30:9–30.

Publisher's Note

Springer Nature remains neutral with regard to jurisdictional claims in published maps and institutional affiliations.